WORKSHOP ON DYNAMICAL PROCESSES ON COMPLEX NETWORKS

May 13-17, 2024

Collective behaviors in neuronal networks under the actions of electric and magnetic fields

Presented by:

SIMO Gaël Rosain

University of Ebolowa, HIGHER TECHNICAL TEACHERS' TRAINING COLLEGE,
University of Dschang, Faculty of Science, Departnment of Physics,
Cameroun

1. Context and motivation of the work

❑ CONTEXT

- To understand and control certain neuronal behaviors.

-Neurological and neurodegenerative diseases (Alzheimer's, Parkinson's, epilepsy, Multiple sclerosis, cerebrovascular accidents, etc.),
-psychiatric diseases (anxiety, depression, addiction, schizophrenia, autism),
-deficiencies of the sense organs (visual and hearing impairments , somesthetics or olfactory) are most affected by research on the brain.

- We live every day accompanied by the electromagnetic fields that surround us.

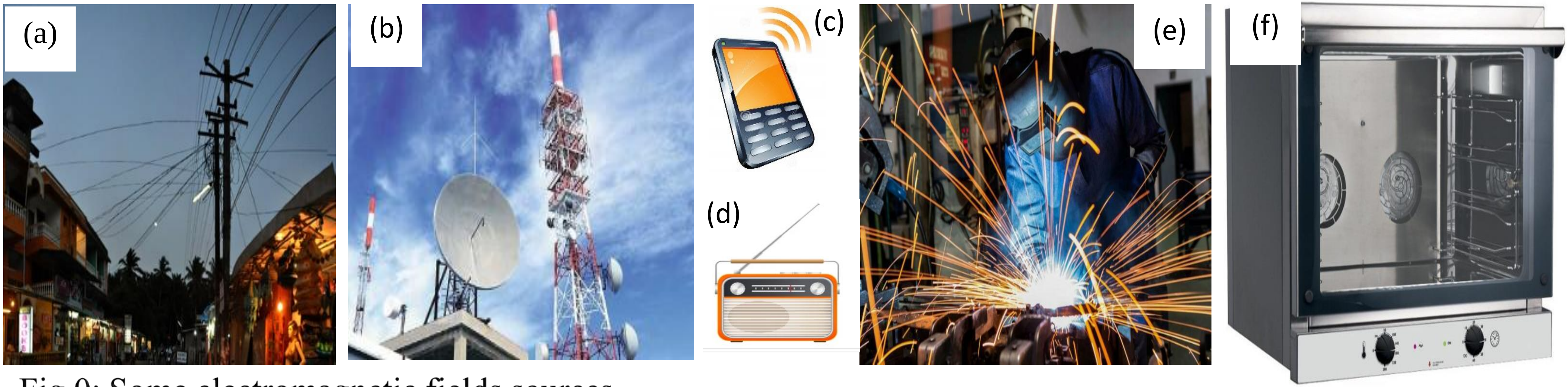

Fig 0: Some electromagnetic fields sources.

❑ MOTIVATION

- The brain as a complex system
- Neuronal synchronization links to several brain pathologies
- Chimera state and similarity in certain animals
- Traveling chimera state as a variant of chimera state

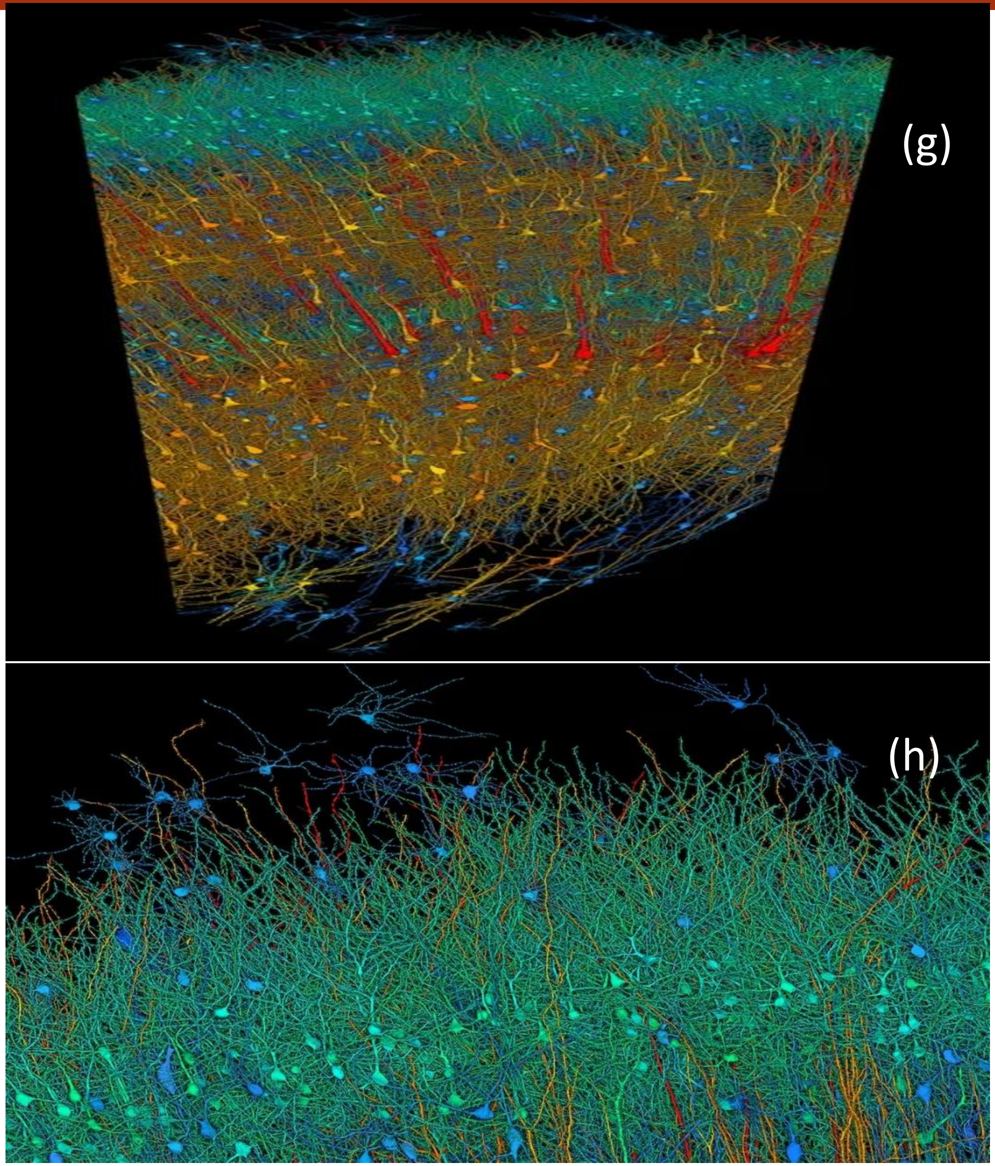

Fig 0: ***Google Research & Lichtman Lab (Université de Harvard)/Rendu par D. Berger***

What would be the influence of the electromagnetic fields on chimera states in a network of Hindmarsh-Rose neurons?

3. What’s Neuron?

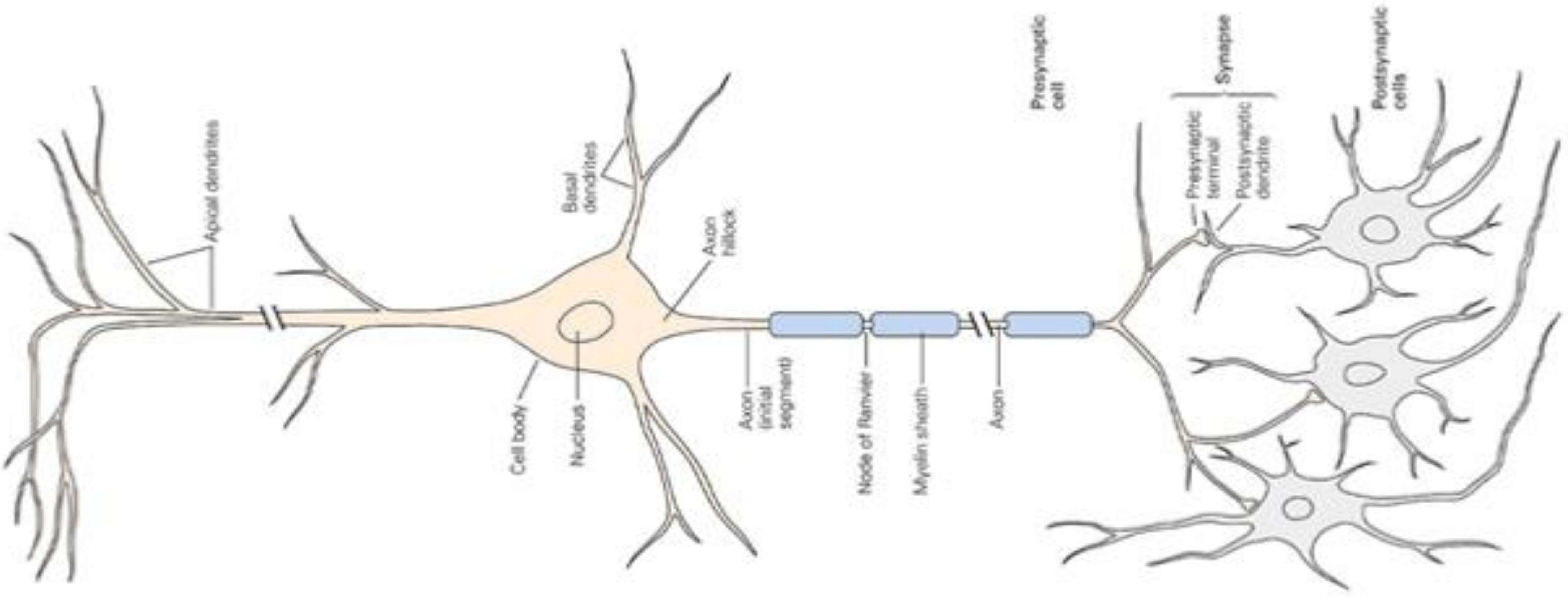

Fig1: Schematic view of a neuron(Kandel et *al*., 1991)

4. HR neuronal models

a)Three-equations model

$$\begin{cases} \dot{x} = y - ax^3 + bx^2 + I - z \\ \dot{y} = c - dx^2 - y \\ \dot{z} = r(s(x - x_0) - z). \end{cases} \quad (1)$$

(Hindmarsh and Rose, 1984)

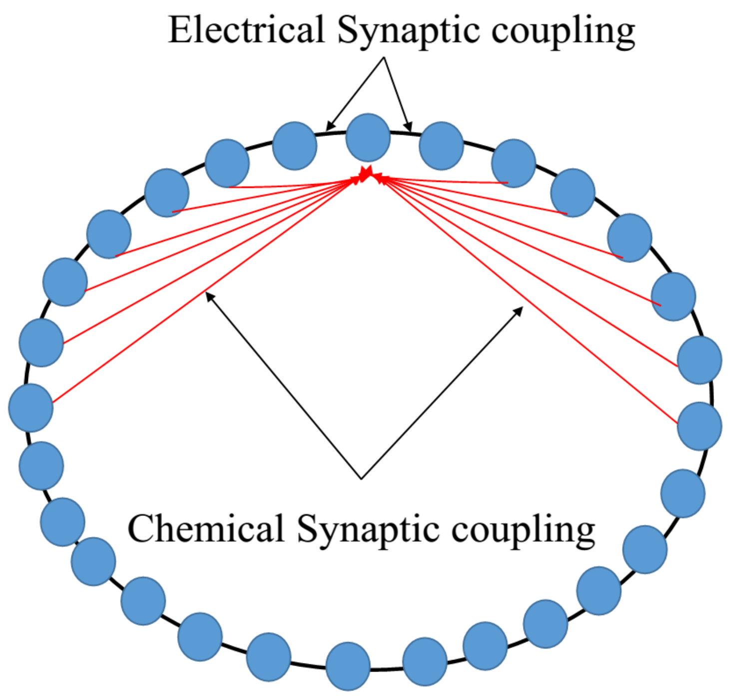

Fig2: Schematic diagram of a neuronal network. Blue dots represent HR neurons connected to their nearest neighbors by local Electrical coupling in black lines. Red lines represent non-local chemical synaptic coupling shown for one node, which is true for all other nodes.

Network Equations

$$\begin{cases} \dot{x}_i = y_i - a x_i^3 + b x_i^2 - z_i + I + J_i + C_i \\ \dot{y}_i = 1 - d x_i^2 - y_i \\ \dot{z}_i = r(s(x_i - x_{i0}) - z_i) \end{cases} \quad (1)$$

$$J_i = k_1 \sum_{j=i-1}^{j=i+1} (x_j - x_i) \quad (2)$$

$$C_i = \frac{k_2}{2p-2}(x_s - x_i)\left(\sum_{j=i-p}^{i+p} \Gamma(x_j) - \sum_{j=i-1}^{i+1} \Gamma(x_j)\right) \quad (3)$$

where $\Gamma(x) = \dfrac{1}{1 + \exp(-\lambda(x - \theta))}$

a) Traveling chimera

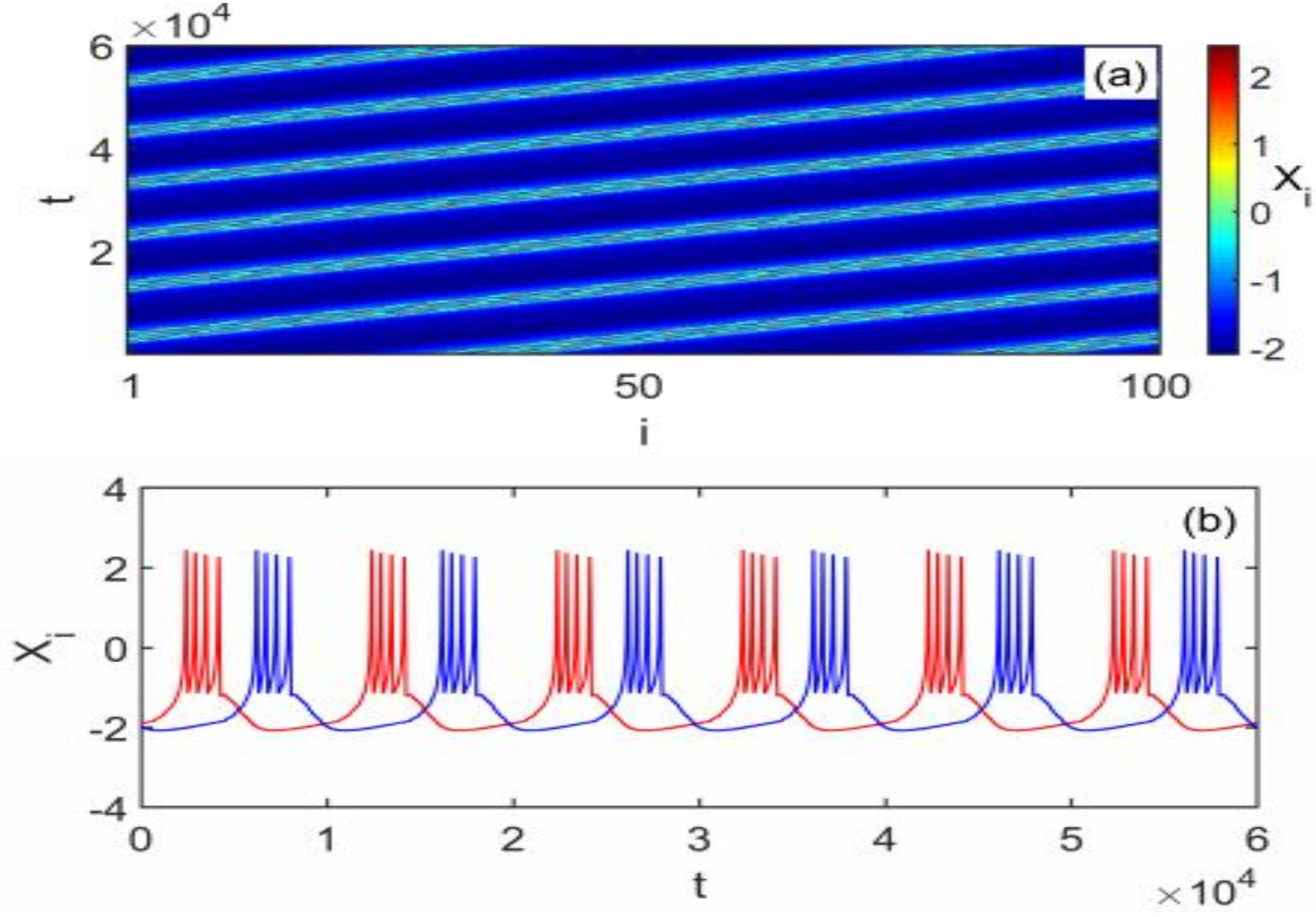

Fig3:Traveling chimera patter n for only chemical synaptic coupling, $k1$ = 0, $k2$ = 9, I = 3.5. (a)Spatiotemporal evolution of xi shows the traveling chimera pattern, where the magnitude of xi is indicated by the color bar; (b) Time series of xi of: node 5 in blue and node 50 in red.

a) Traveling chimera

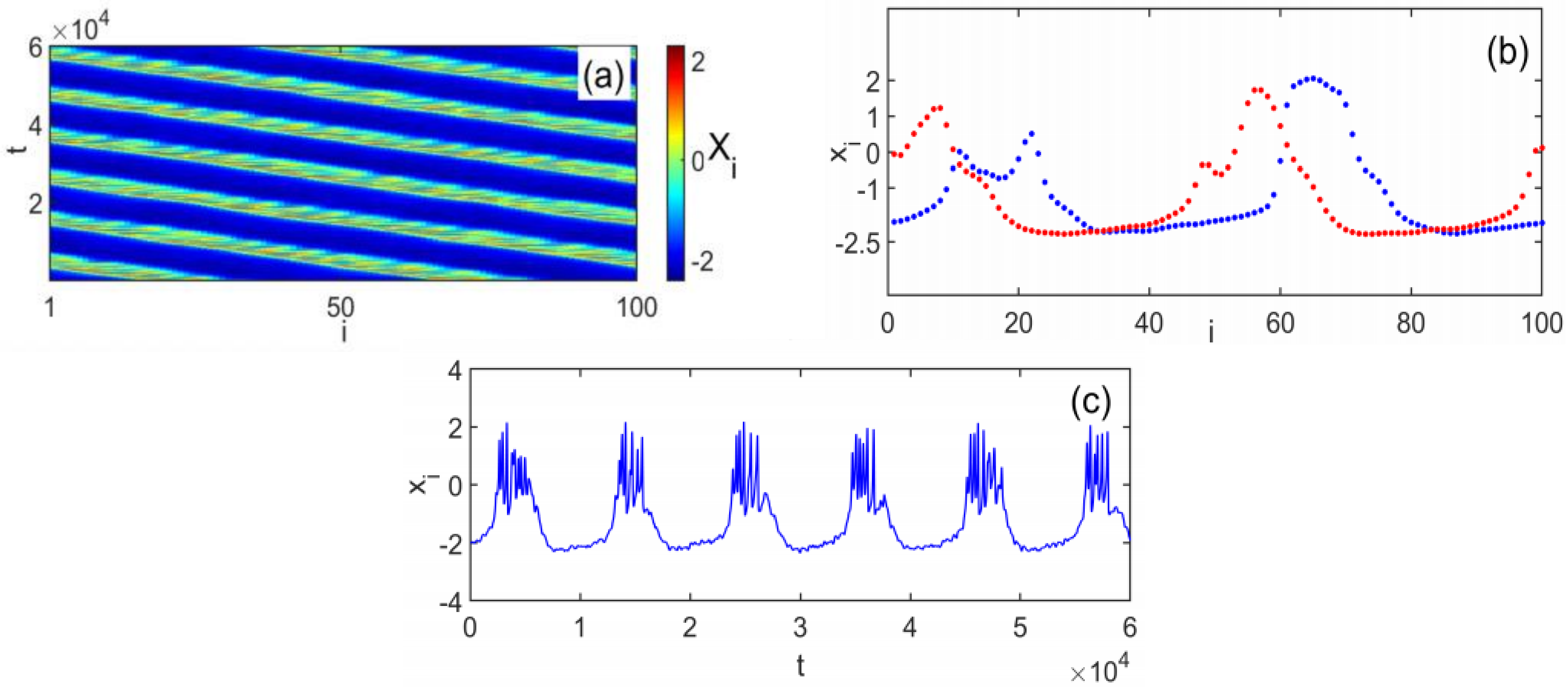

Fig4:Traveling chimera patter n for $k2 = 4$, $k1 = 3$, $I = 3.5$. (a) Spatiotemporal evolution of xi where the magnitude of xi is indicated by the color bar. The pattern travels from bottom left to upper right corner in time.(b) Snapshots of xi of all nodes at two different instants. (c)Time series shows a chaotic bursting behavior.

6. Phenomenon appearing in 1D-NN

b) Impact of *p*: the number of neighbors into chemical connections.

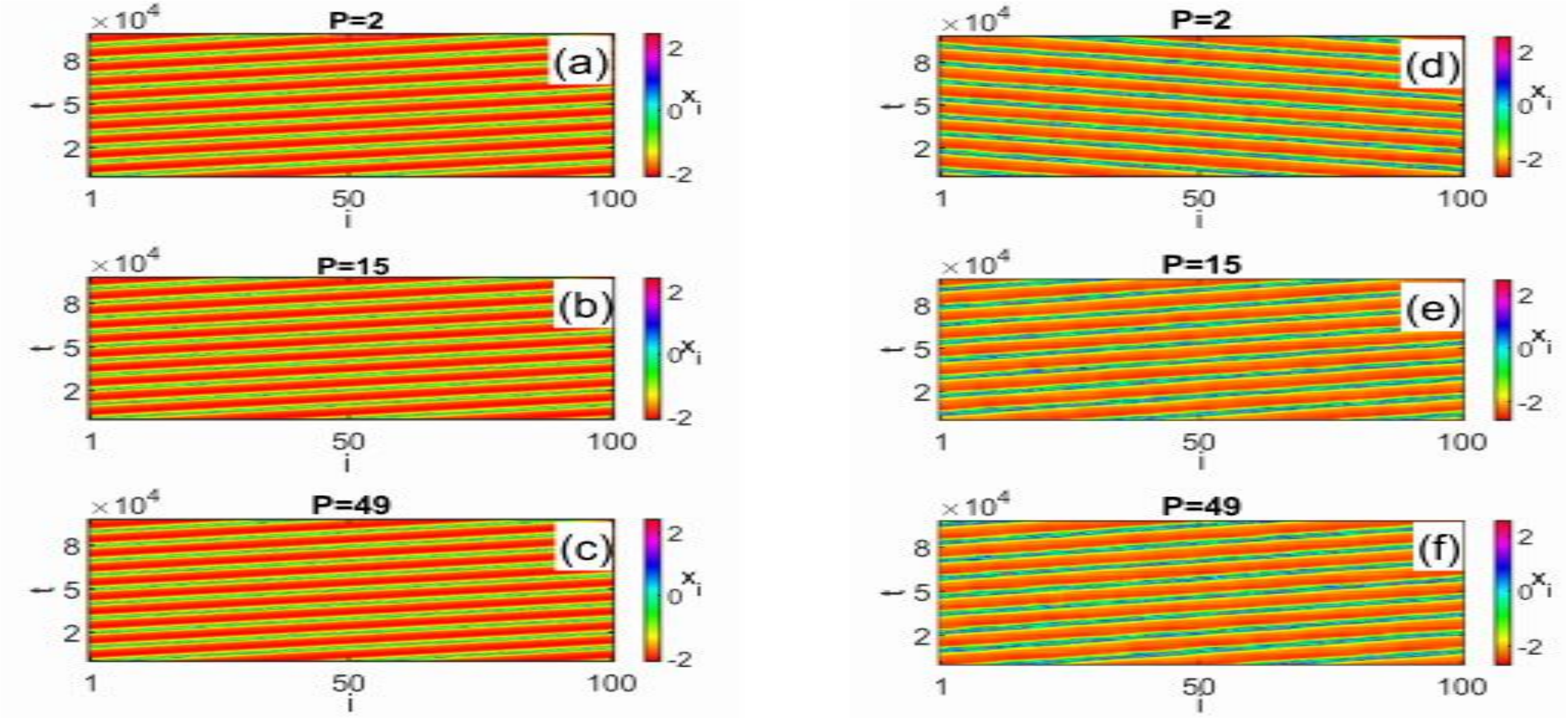

Fig5: Role of the number of neighbors *p* on the dynamics of the network's traveling chimera (a), (b), (c) without electrical coupling ($k1 = 0$, $k2 = 9$); (d), (e), (f) with electrical coupling ($k1 = 1$, $k2 = 9$

c)Traveling speed's estimation for the traveling chimera state

$$J_{x\max}(t) = j\max\{x_1(t), x_2(t), \ldots, x_N(t)\} \quad (4)$$

$$v_{tr} = N/T_{tr} = Nf_{tr} \quad (5)$$

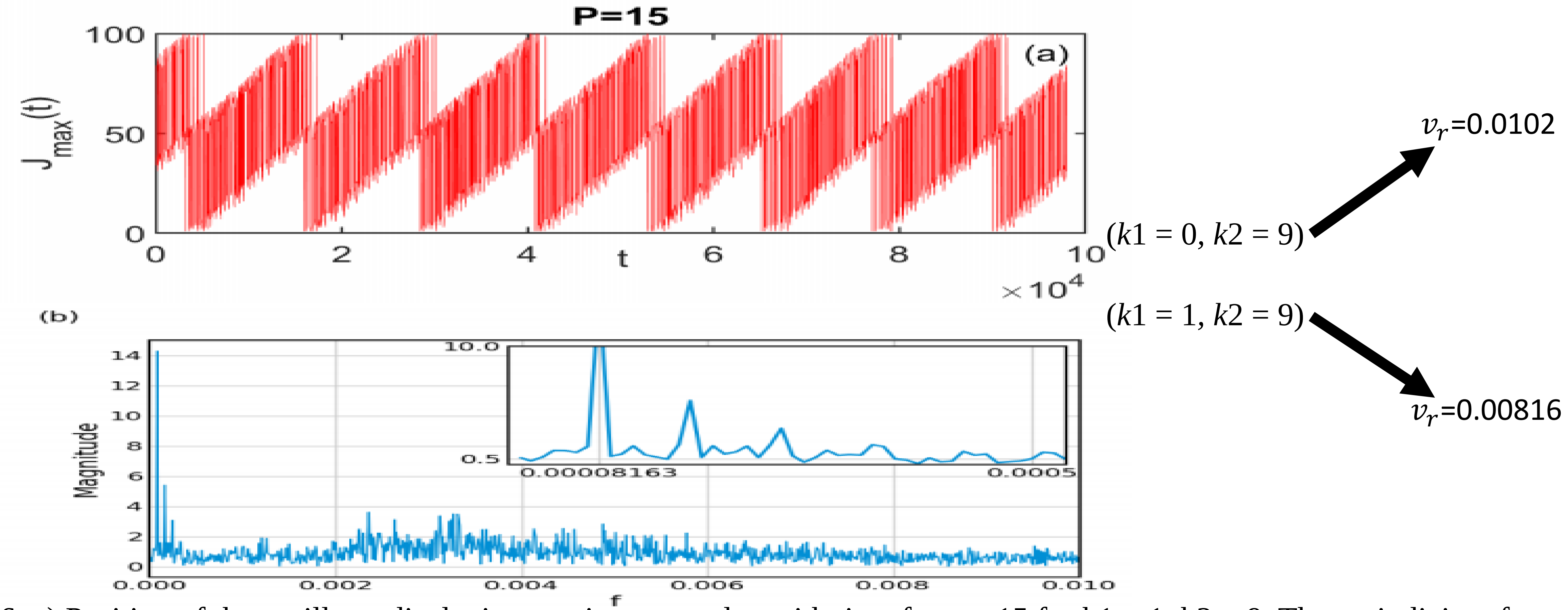

Fig6: a) Position of the oscillator displaying maximum *x*-value with time for *p* = 15 for k1 = 1, k2 = 9. The periodicity of the waveform refers to that of the traveling chimera state. (b) Fourier transforms of *Jmax*(*t*), with low frequencies, expanded in the inset, to discern the frequencies of the traveling motion around the ring (*ftr* = 0.0000816).

d) Multicluster and traveling multicluster chimera breathers.

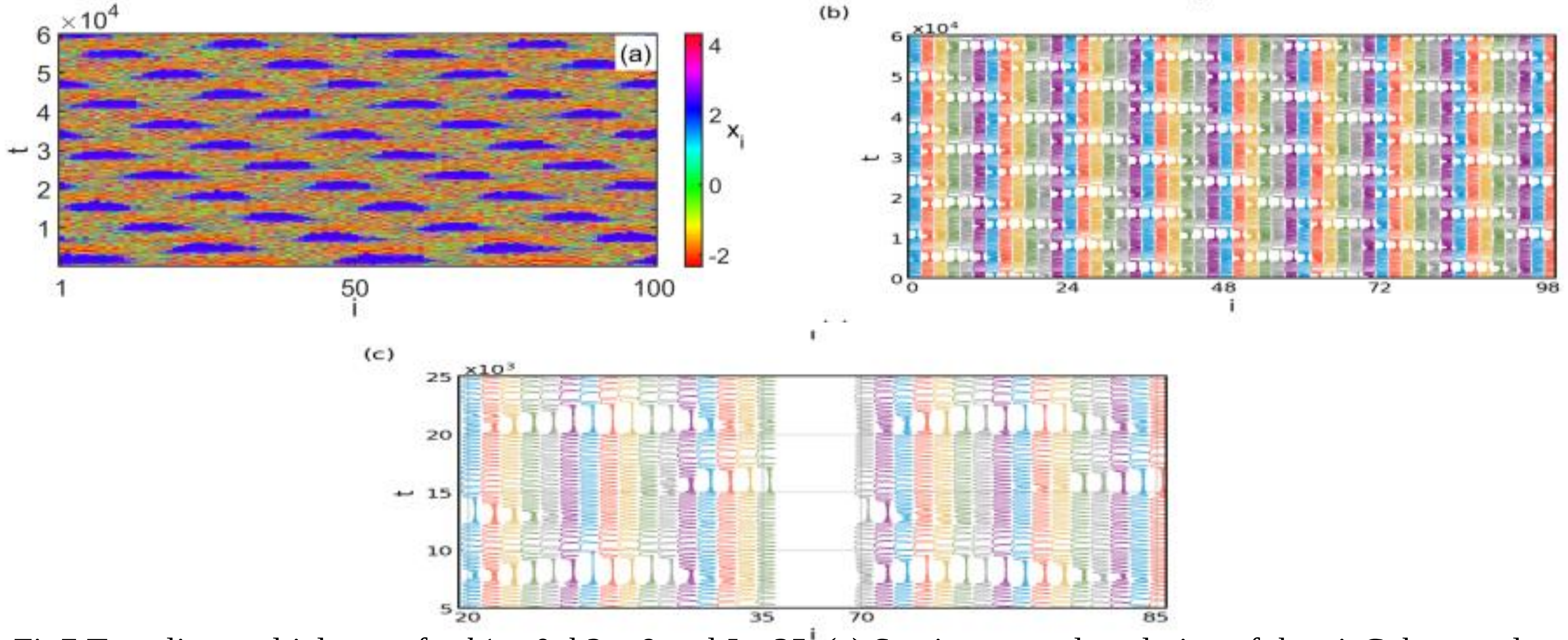

Fig7:Traveling multiclusters for $k1 = 0$, $k2 = 9$ and $I = 35$. (a) Spatiotemporal evolution of the x_i. Coherent clusters in blue. (b) Plot of time series of neurons with even index i for better visualization of coherent clusters. (c) Close up on figure (b), where the coexistence of coherent regions, marked by low-frequency behavior, is distinctly seen.

e) Multicluster and traveling multicluster chimera breathers.

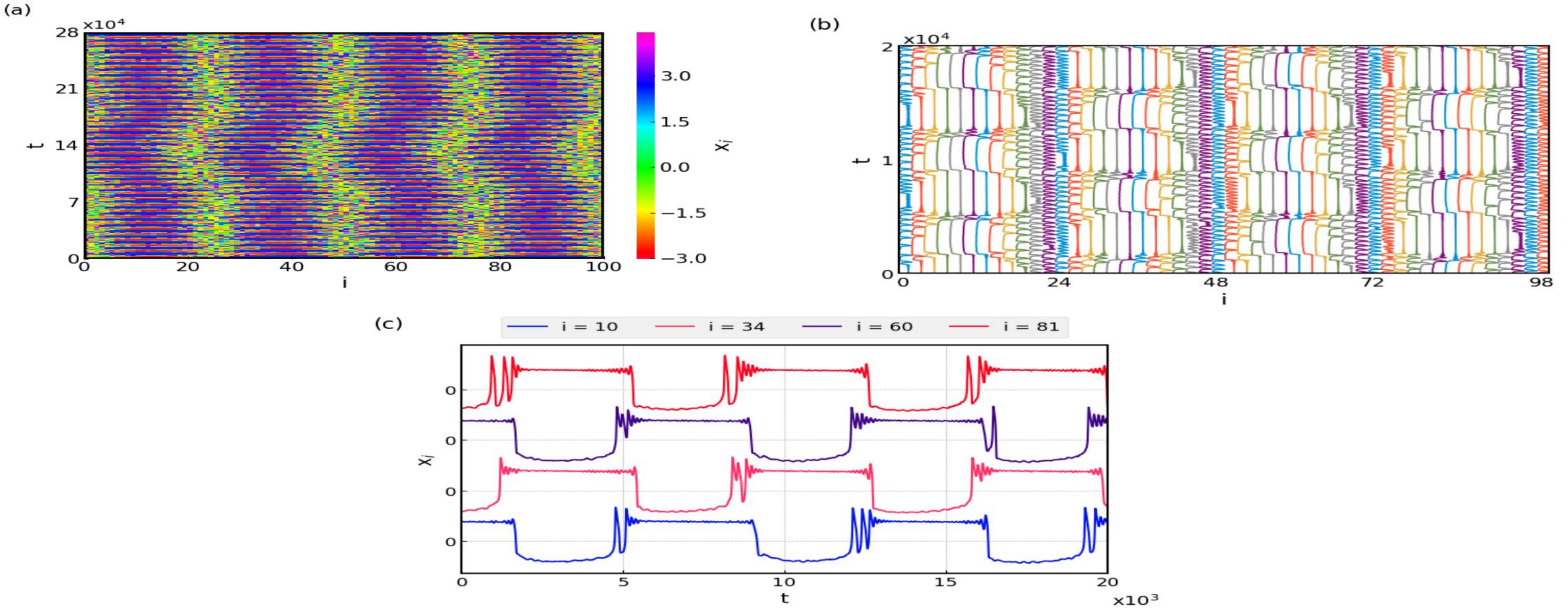

Fig8:Multicluster chimera breathers, for *k*1 = 0, k2 = 10, *I* = 35. (a) Spatiotemporal evolution of *xi*, marked by four coherent regions. (b) Close-up of (a), details of *xi* show the existence of multiclusters. (c) Time-series of *xi* for neurons inside different but subsequent clusters show that these present an “antiphase” like behavior.

f)Local Order Parameter in one dimension

$$L_i = \left| \frac{1}{2\eta} \sum_{|i-k| \le \eta} e^{j\phi_k} \right| \qquad (6)$$

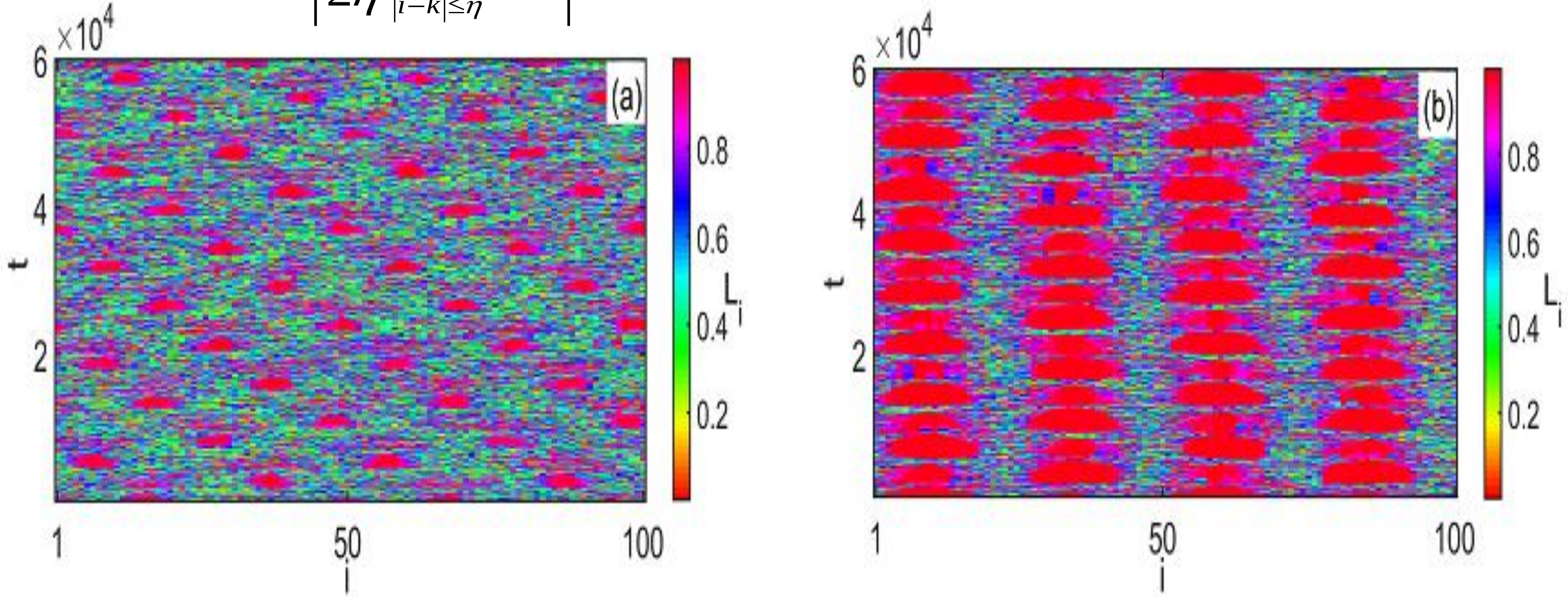

Fig9: Spatiotemporal evolution of the local order parameter *Li* with $\eta = 2$, the magnitude of *Li* is indicated using color bars: (a) For the parameters of Fig.10; (b) For the parameters of Fig.11.

Network Equations

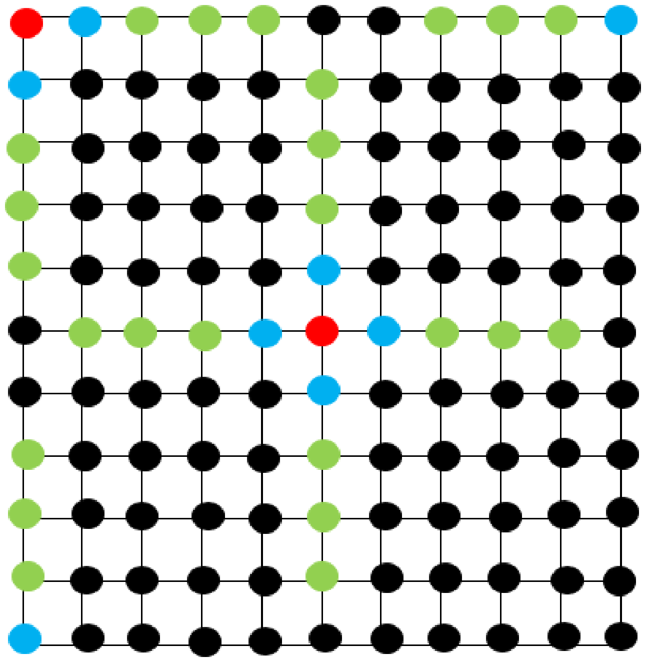

Fig10: Schematic diagram of a two-dimensional grid: the (i, j)-th node (red dot) is locally connected to four nearest-neighbors (blue circles) and non-locally connected to $p$nearest-neighbors (green circles). Black circles represent other nodes on the network. For the simple illustration, we choose M = 11 and p = 3

$$\begin{cases} \dot{x}_{i,j} = y_{i,j} - a x_{i,j}^{3} + b x_{i,j}^{2} - z_{i,j} + I + J_{i,j} + C_{i,j}, \\ \dot{y}_{i,j} = 1 - d x_{i,j}^{2} - y_{i,j}, \\ \dot{z}_{i,j} = r(s(x_{i,j} - x_{i,j0}) - z_{i,j}). \end{cases} \quad (7)$$

$$J_{i,j} = \frac{k_1}{4}\left(\sum_{l=i-1}^{i+1}\left(x_{l,j} - x_{i,j}\right) + \sum_{l=j-1}^{j+1}\left(x_{i,l} - x_{i,j}\right)\right) \quad (8)$$

$$C_{i,j} = \frac{k_2}{4p-4}\left(v_s - x_{i,j}\right)\left(\sum_{\substack{l=i-p \\ p\neq 0,1}}^{i+p}\Gamma\left(x_{l,j}\right) + \sum_{\substack{l=j-p \\ p\neq 0,1}}^{j+p}\Gamma\left(x_{i,l}\right)\right). \quad (9)$$

a) Traveling chimera state in 2D-NN

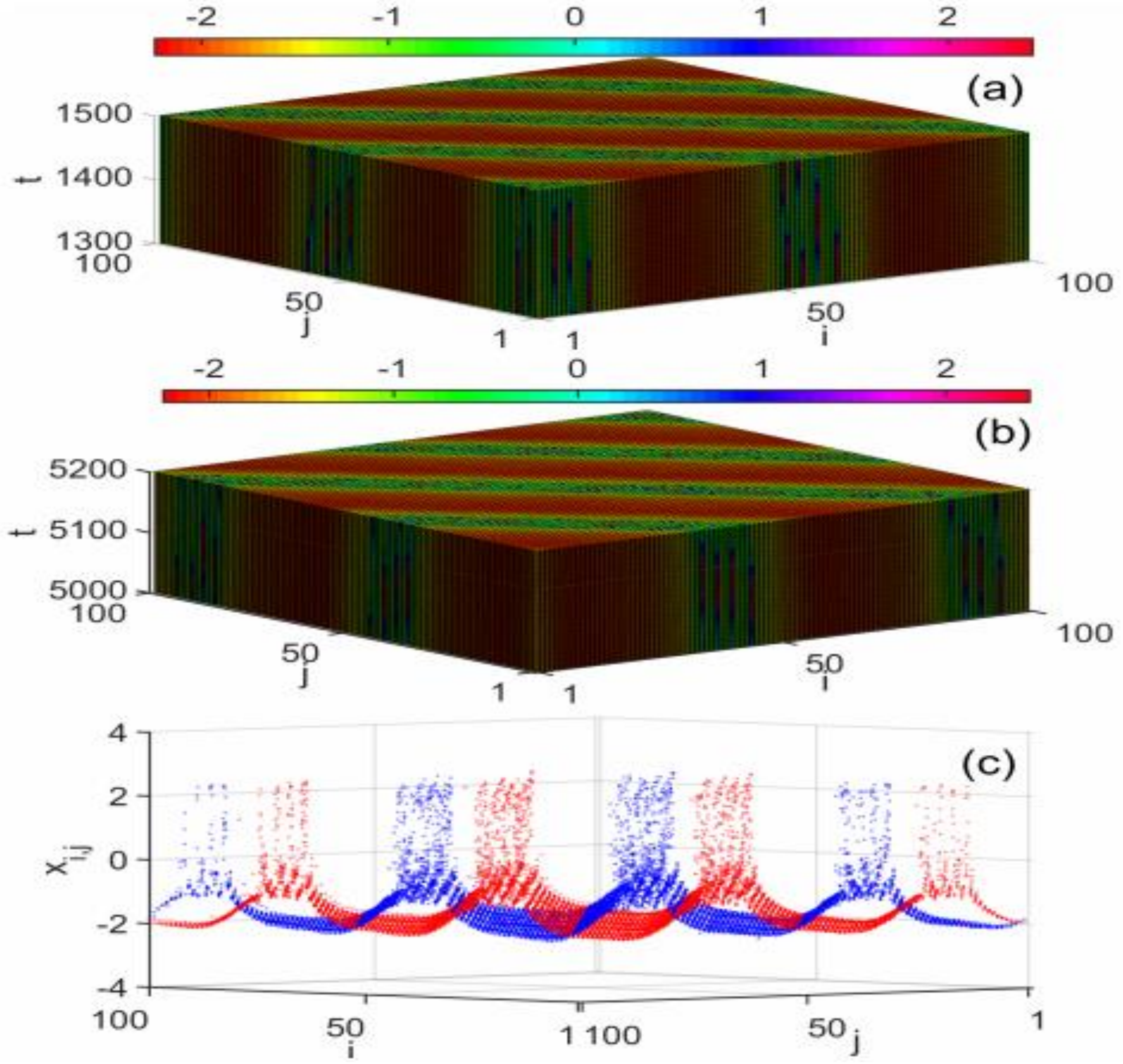

Fig11:Traveling chimera patterns in 2D network for synaptic coupling $k2 = 9$ ($k1 = 0$). (a,b) Spatiotemporal evolution of xi,j for $M2$ neurons, (c) snapshots of $M2$ number of xi,j variables in 2D plane at two different instant of times. Blue curve is for a later time than the red snapshot implying a traveling pattern. The color bars in (a, b) represent the variation of xi,j.

a) Traveling chimera state in 2D-NN

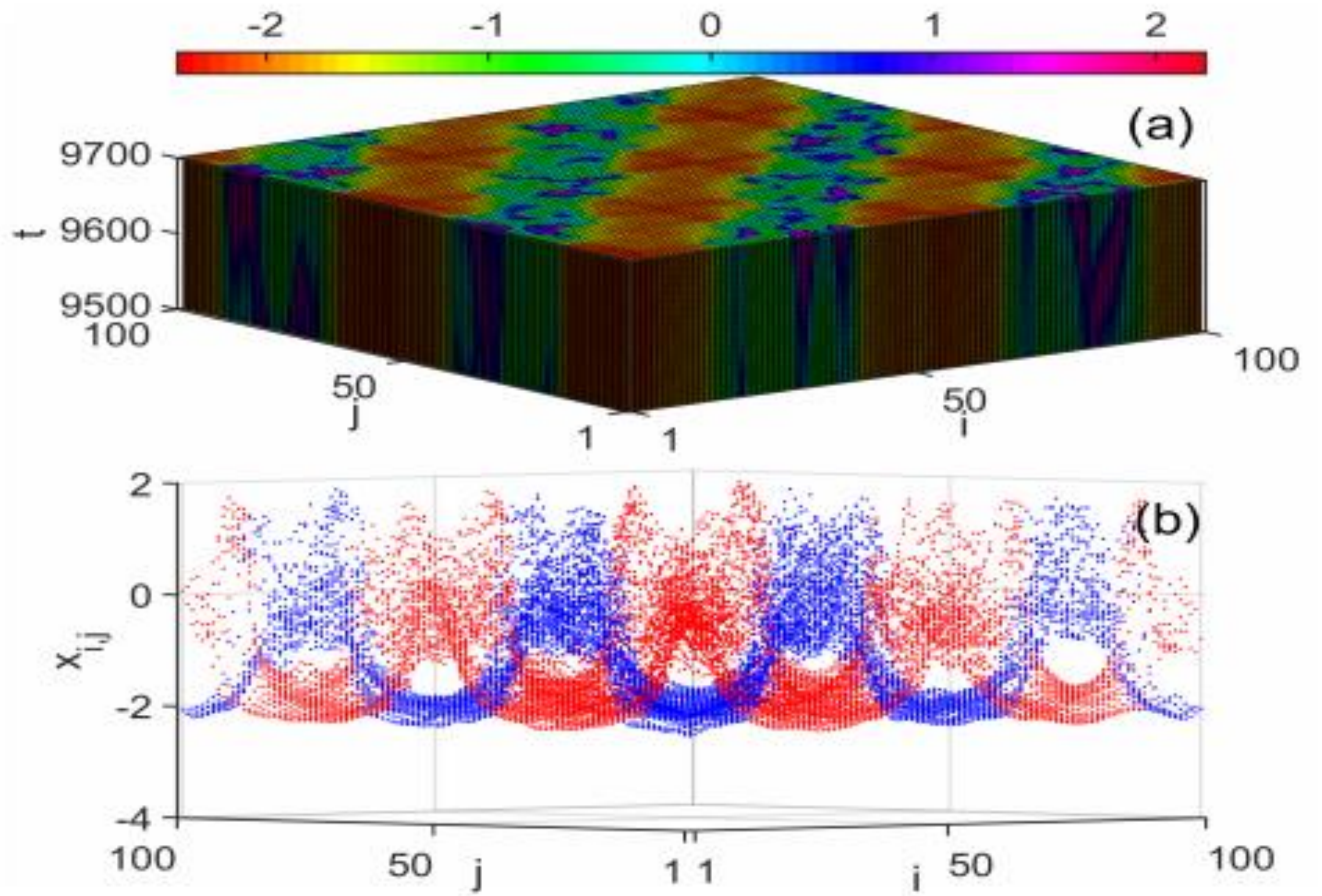

Fig12:Traveling chimera patterns in 2D network for synaptic coupling $k1= 2$ and electrical coupling $k2 = 3$.(a) Spatiotemporal evolution of $x_{i,j}$ for $M2$ neurons, b)snapshots of the $M2$ $x_{i,j}$ variables in two differents instant of times. Blue curve is for a later time than the red snapshot implying a traveling pattern.

7. Phenomenon appearing in 2D-NN

a) Traveling chimera state in 2D-NN

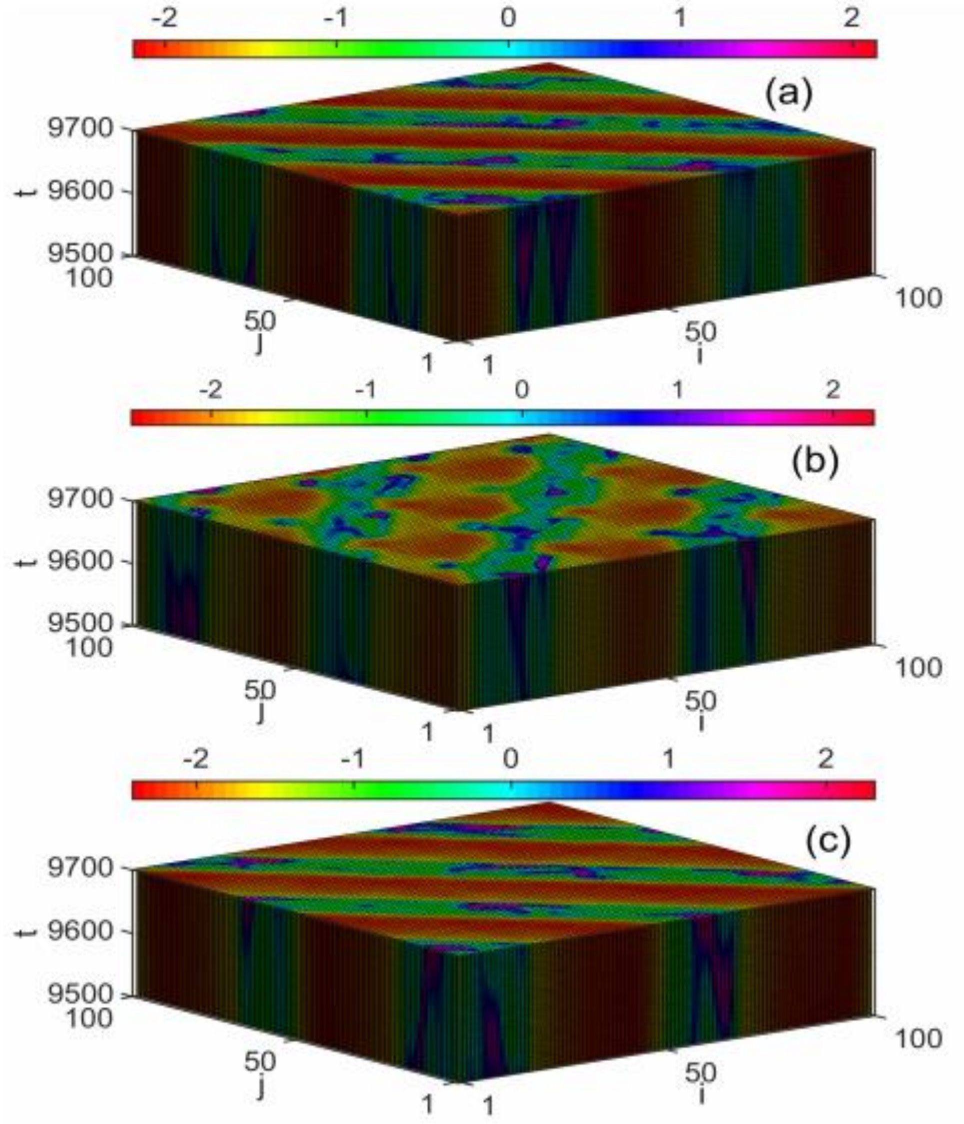

Fig13: Traveling chimera patterns in 2D network for synaptic and electrical coupling with $k1 = 5$, (a) $k2 = 2.5$, traveling chimera state, (b) $k2 = 2.75$, imperfect traveling chimera patterns, (c) $k2 = 3$, traveling chimera state. Here, the direction of traveling pattern in (b) changes with the direction of (a, c).

b) Traveling Multi-clusterin 2D-NN

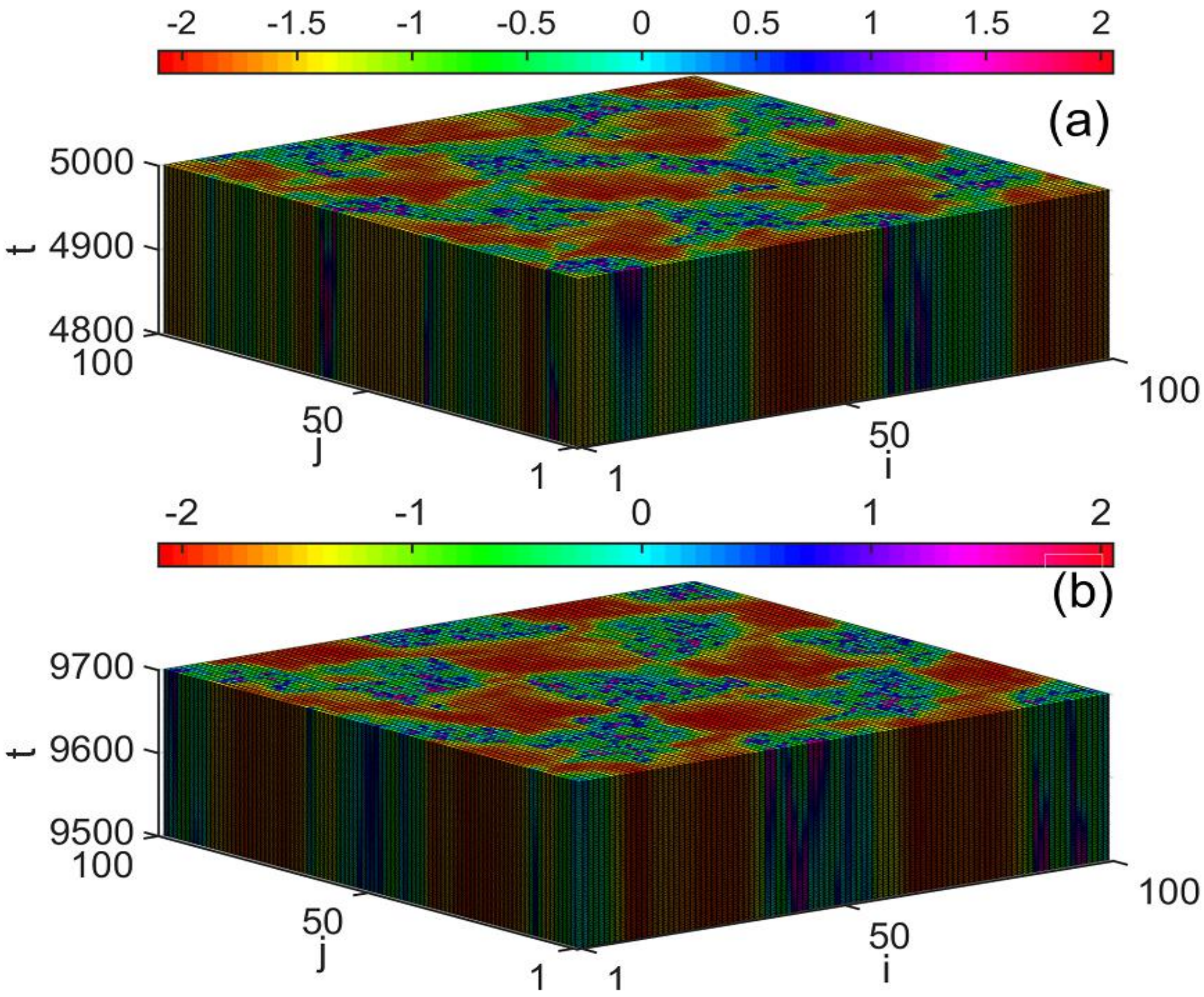

Figure 14: Traveling multi-cluster in 2D network for electrical coupling $k1 = 1$ and synaptic coupling $k2 = 1$. (a,b) spatiotemporal evolution of xi,j for $M2$ neurons at two different times.

c) Alternating Traveling Chimera state in 2D-NN

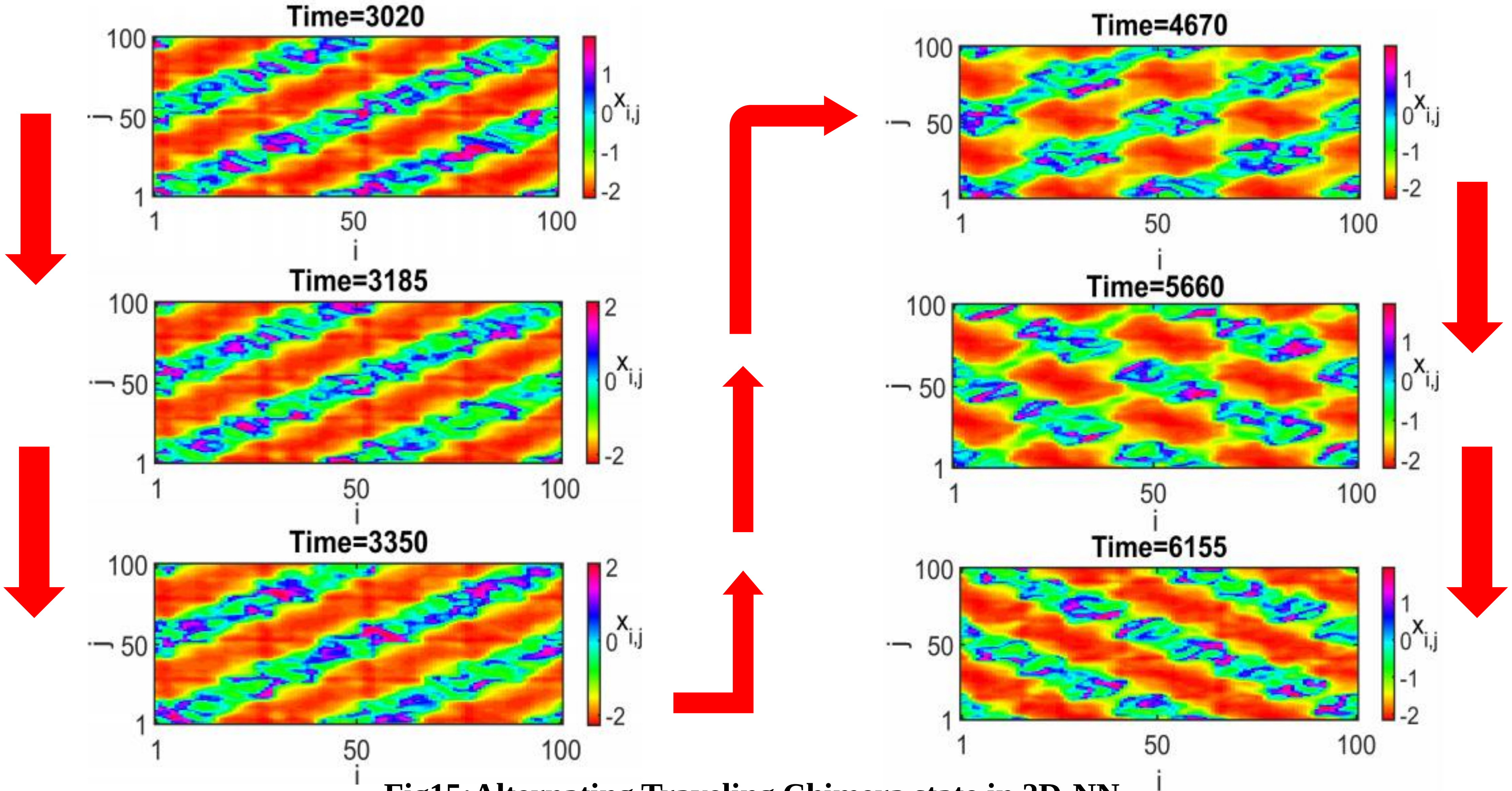

Fig15:Alternating Traveling Chimera state in 2D-NN

c) Alternating Traveling Chimera state in 2D-NN

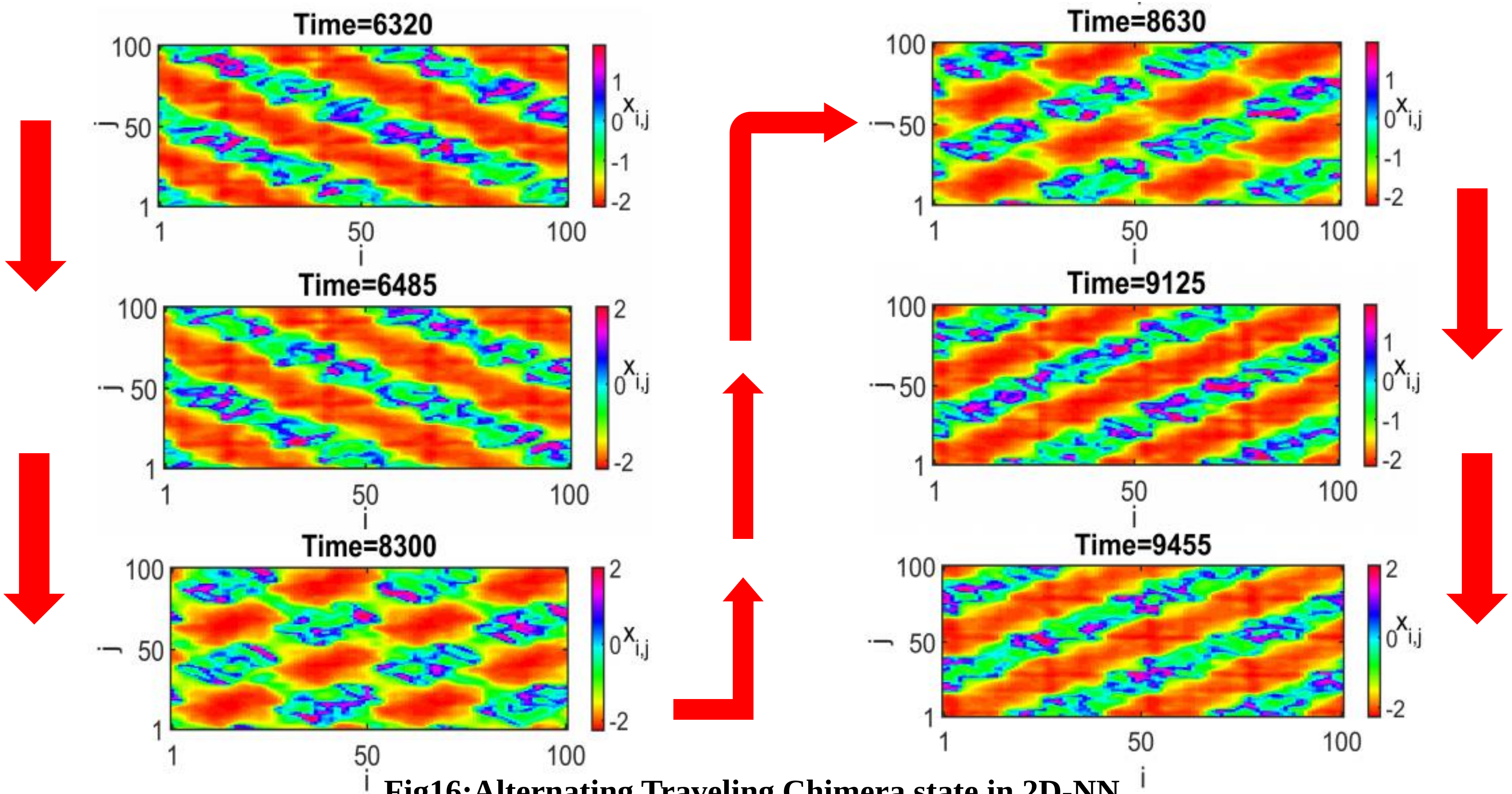

Fig16:Alternating Traveling Chimera state in 2D-NN

3. Confirmation of coherent states by using 2D-LOP

$$L_{i,k} = \left| \frac{1}{(2\eta+1)^2} \sum_{|i-\alpha|\le\eta} \sum_{|k-\beta|\le\eta} e^{j\Phi_{\alpha,\beta}} \right| \quad (10)$$

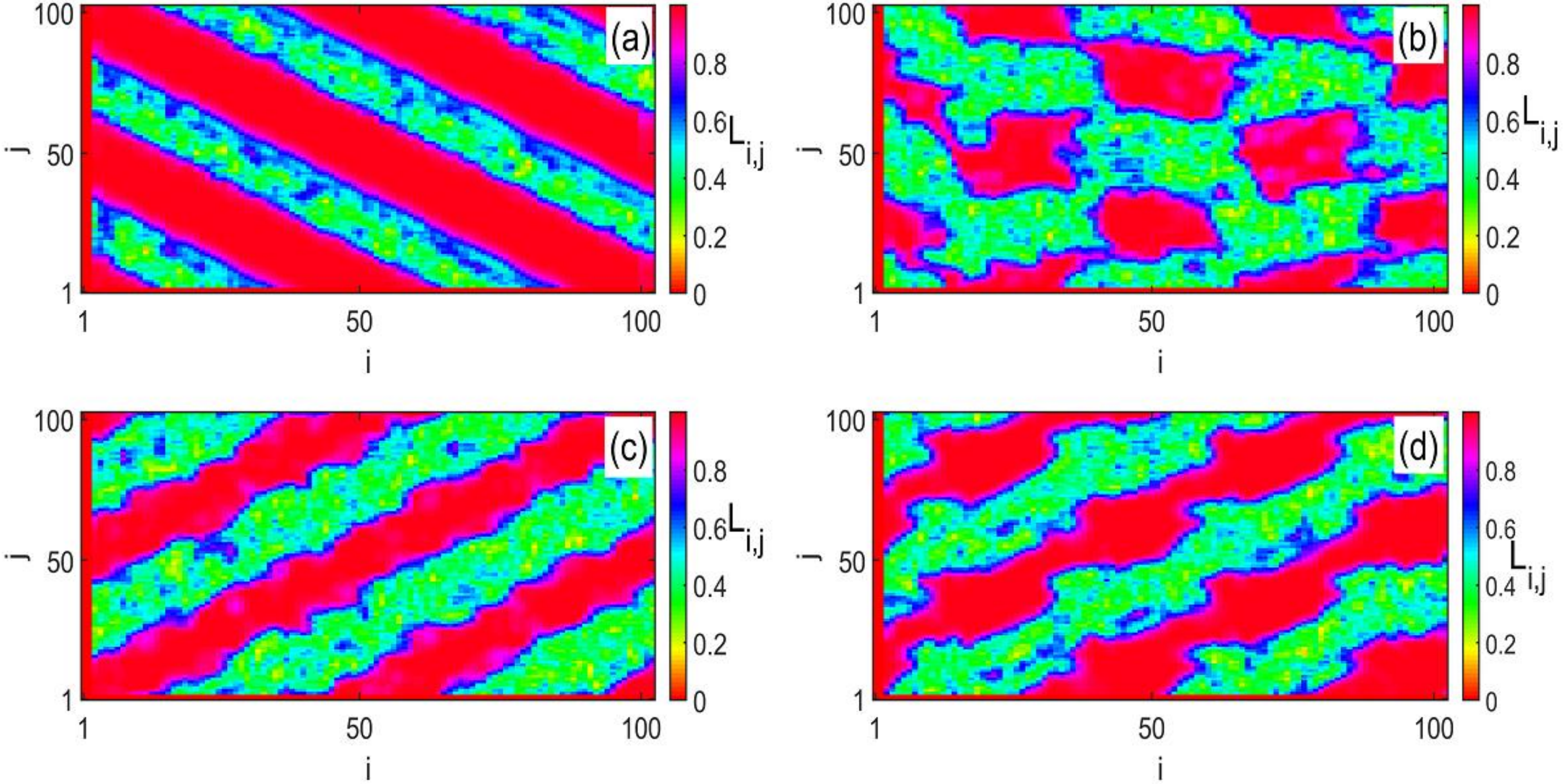

Figure 17: The var iation of the 2D local order parameter at a numer ical time t = 9700: corresponding coupling strengths (a) $k1$ = 0, $k2$ = 9, (b) $k1$ = 1, $k2$ = 1, (c) $k1$ = 3, $k2$ = 2 and (d) $k1$ = 5, $k2$ = 2.75.

e) 2D Network Energy analysis

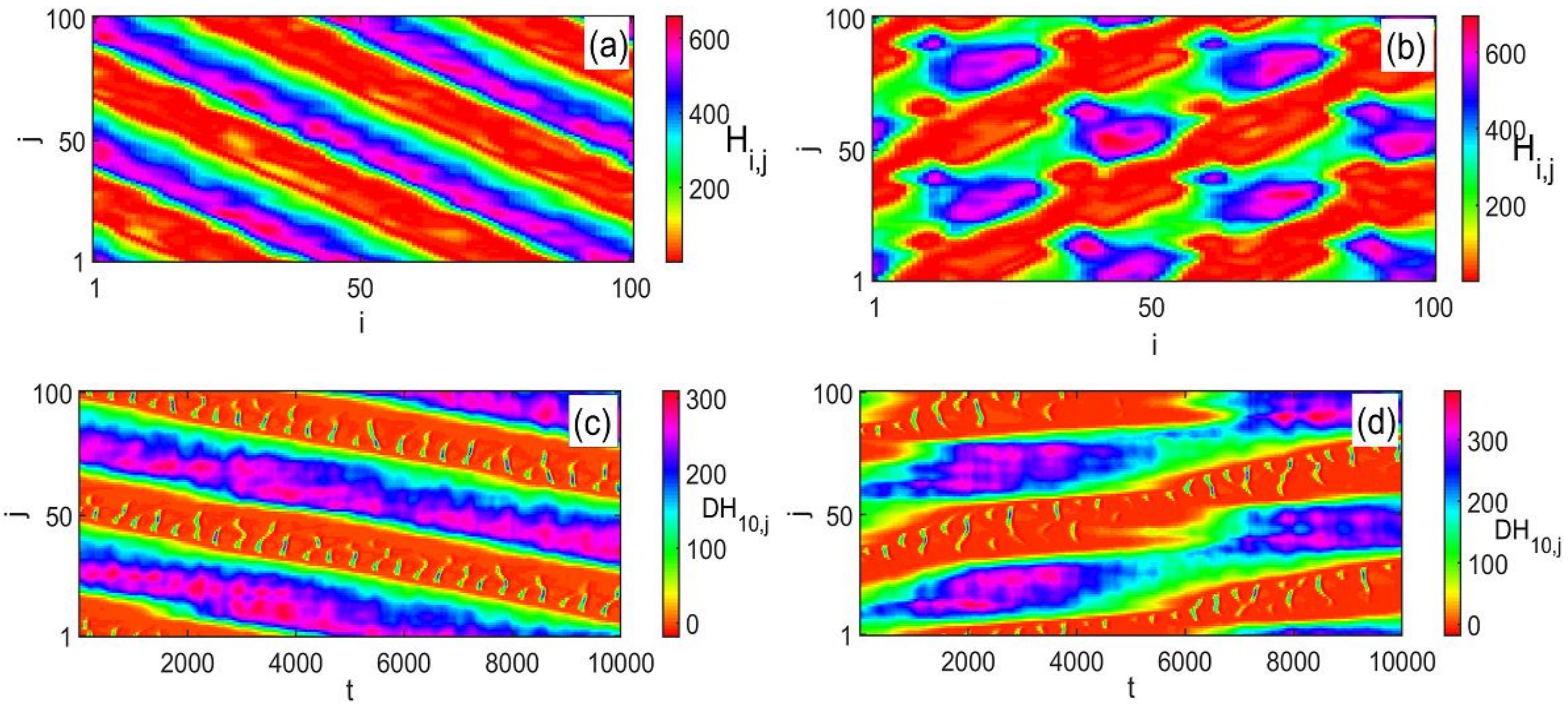

Figure 18: Variation of energies in the 2D plane of the 2D neuronal network at *t*=9700,and the temporal evolution of the derivative energies *DHi,j* of the cross-section defined by (*i* = 10, *j* = 1, ..., *M*). (a, c) *k*1 = 5, *k*2 = 2.5, and (b, d) *k*1 = 5, *k*2 = 2.75.

$$\begin{cases} \dot{x}_i = y_i - a x_i^3 + b x_i^2 - z_i + I + J_i + C_i \\ \dot{y}_i = 1 - d x_i^2 - y_i + k_i E_i \\ \dot{z}_i = r(s(x_i - x_{i0}) - z_i) \\ \dot{E}_i = k_2 y_i + E_{ext} \end{cases} \quad (11)$$

Where $E_{ext} = E_{\max} \sin(2\pi f t)$ (12)

(Ma et al., 2019).

Strength of Incoherence (SI) and Discontinuity Measure (DM)

$$\sigma(m) = \left\langle \sqrt{\frac{1}{n} \sum_{j=n(m-1)+1}^{nm} \left[z_j - \bar{z} \right]^2} \right\rangle_t \quad (13)$$

$$SI\_or\_S = 1 - \frac{\sum_{m=1}^{M} s_m}{M} \quad (14)$$

With $s_m = \Theta(\delta - \sigma(\mathrm{m}))$

$$DM\_or\_\eta = \frac{\sum_{i=1}^{M} |s_i - s_{i+1}|}{2}, (s_{M+1} = s_1) \quad (15)$$

Table I: Characterization of chimera and multichimera states (Gopal *et al.*, 2014).

Dynamical state	(S, η)	Remarks
Coherent	(0,0)	
Chimera	(c,1)	0<c<1
Multichimera	(c,d)	$2 \leq d \leq M/2$
Incoherent	(1,0)	

a) Bursting death and chimera states

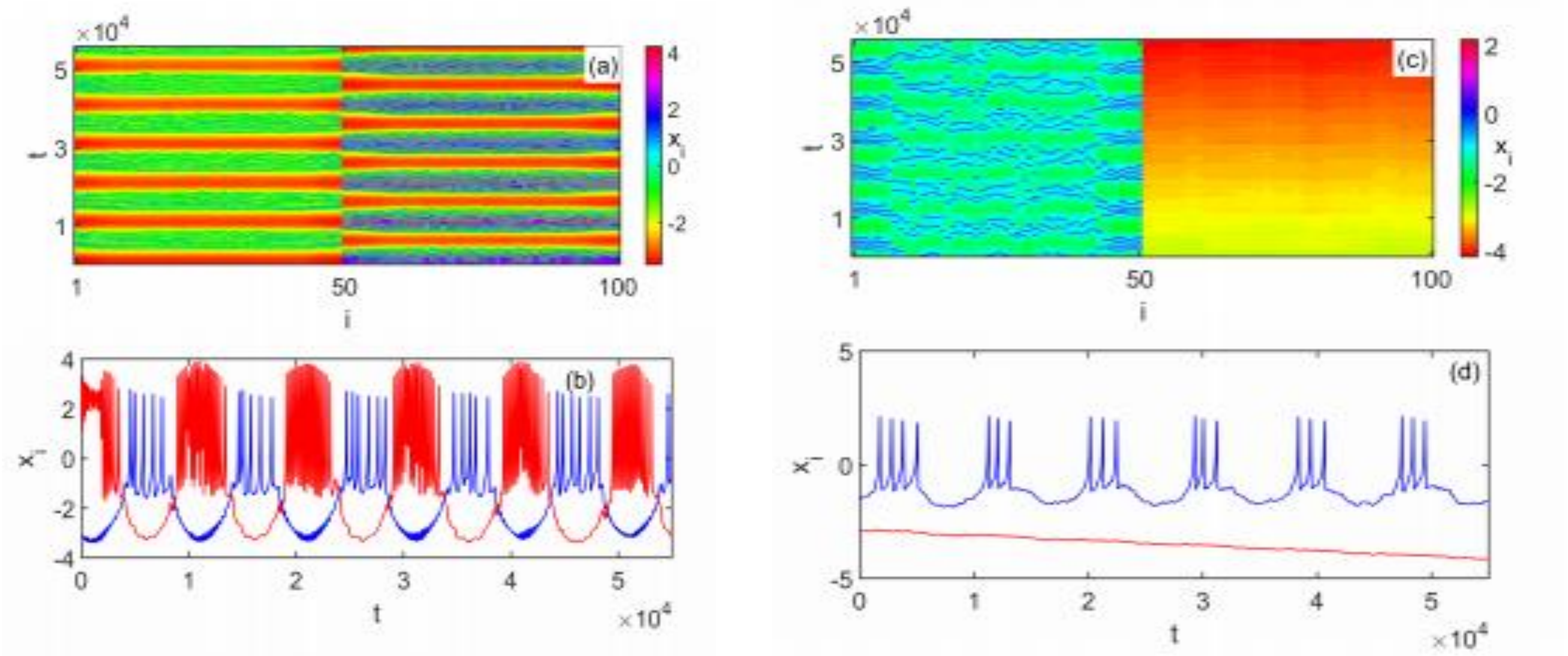

Fig19: Influence of frequency *f*: For *f* = 0.01: (a) Spatio-temporal evolution of the *x*variables; (b) time series of the *x*-variables for neurons in the immersed(red) and non-immersed (blue) regions, where color bars show the amplitude values of the x-variables, For *f* = 12: (c) Spatio-temporal evolution of the *x*-variables; (d) time series of the *x*-variables for neurons in the submerged (red) and non-submerged (blue) regions. Color bars show the amplitude values of x-variables.

b) Influence of the number of subjected elements N

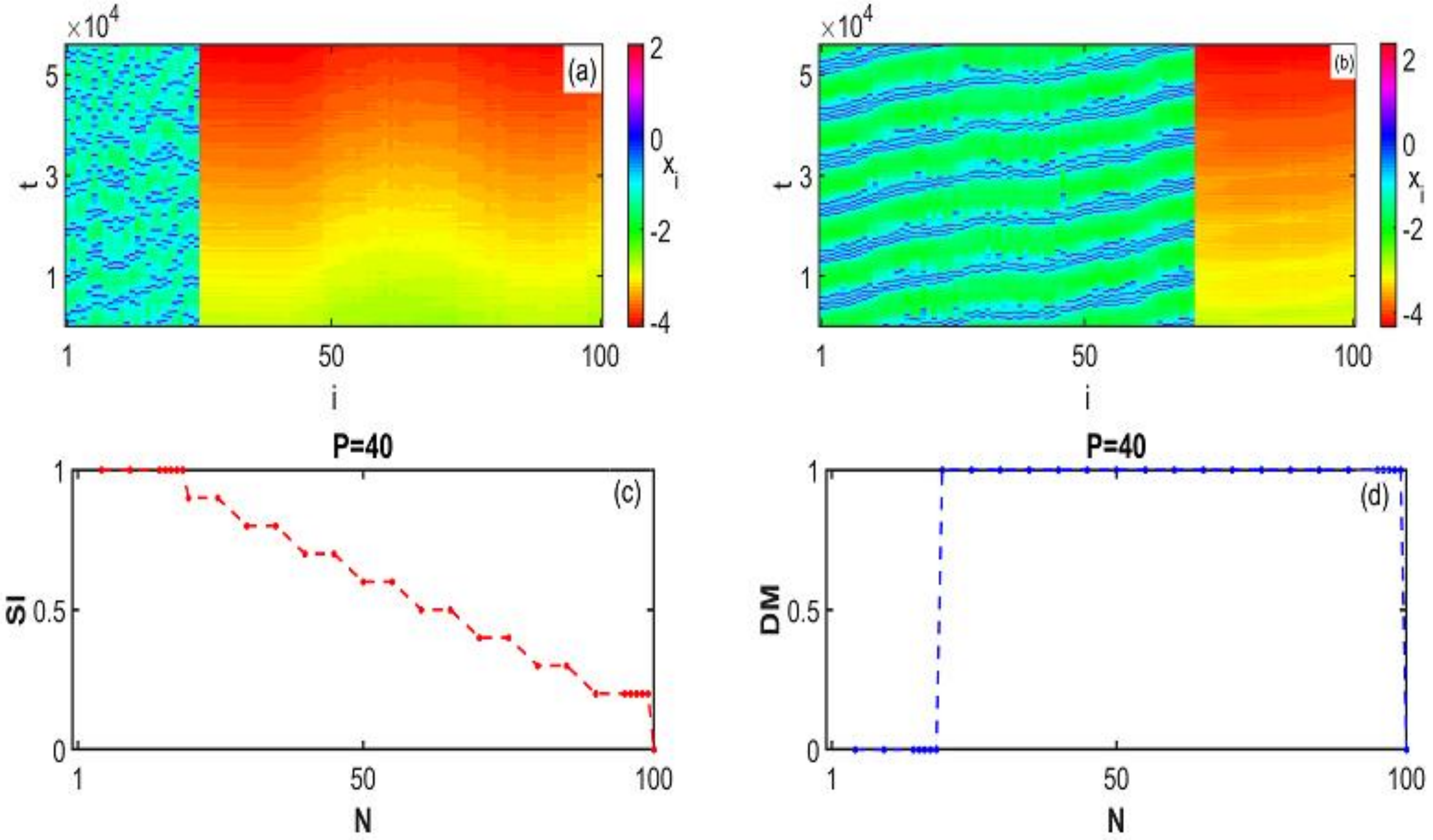

Dynamical state	(S,η)	Remarks
Coherent	(0,0)	
Chimera	(c,1)	0<c<1
Multichimera	(c,d)	$2 \leq d \leq M/2$
Incoherent	(1,0)	

Fig20: Influence of the number of neurons *N* subjected to the external electric field with the frequency *f* = 12. (a) For *N* = 75, spatiotemporal evolution for all the nodes, where we observe a chimera state for the first non-immersed 25 neurons; (b) Imperfect traveling chimera in the non-submerged zone; (c) Strength of incoherence *SI* and (d) Discontinuity Measure *DM* as a function of *N*. Chimera state appears from *N* = 20.

c) Multichimera state

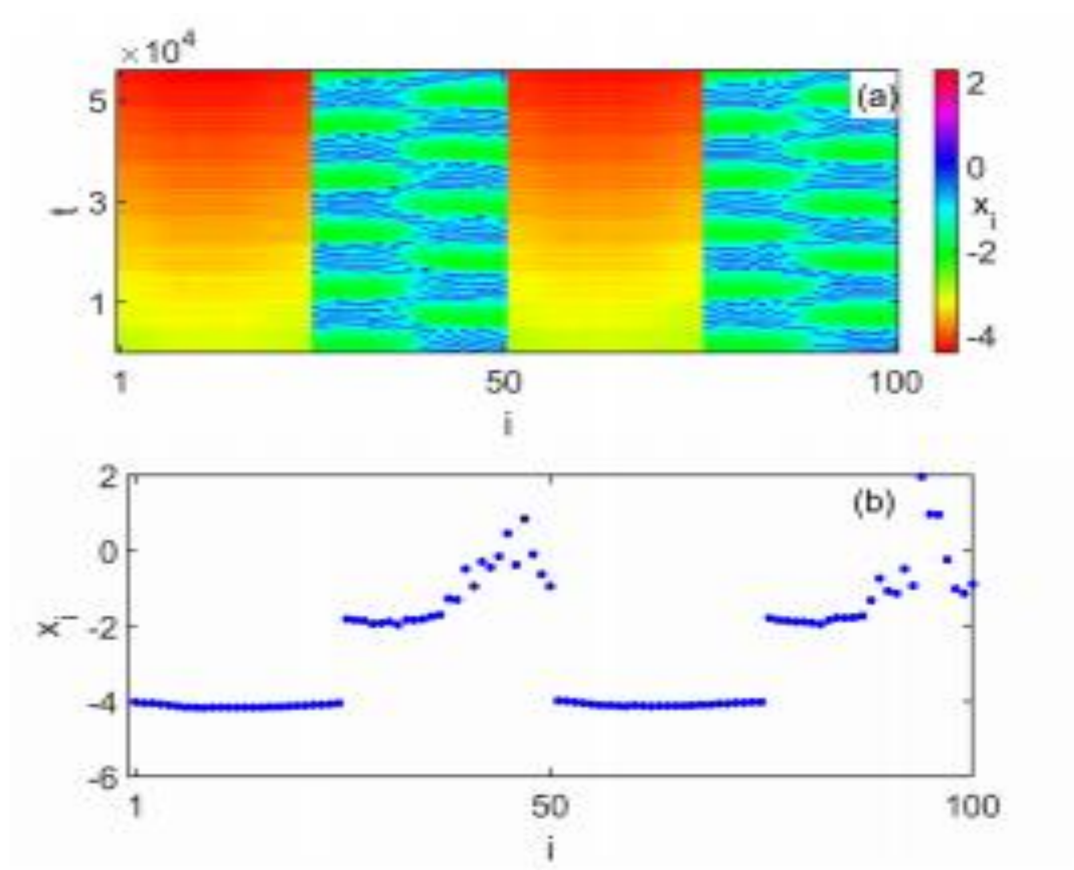

Fig21: (a) Multichimera state induced by application of an electr ic field in two nonconsecutive regions ($q1 = 0$ and $q2 = 9$); (b) Correspondent snapshot of the var iables *xi*

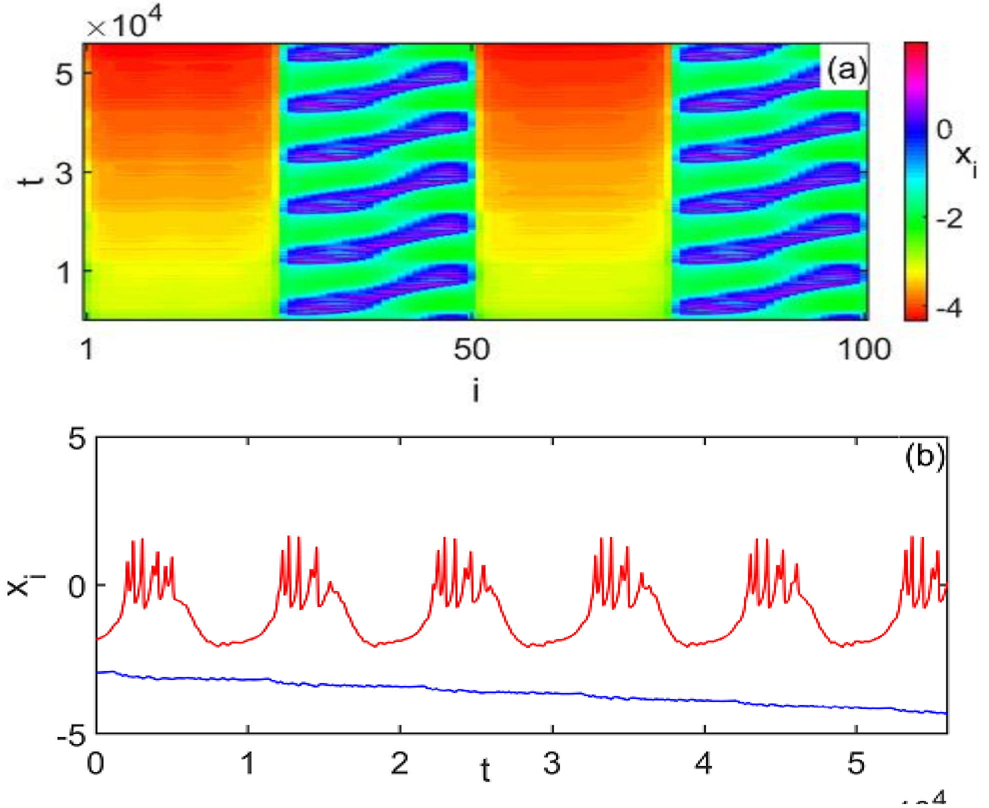

Figure 22: Impact of electrical coupling ($q1 = 2$ and $q2 = 3$) for f =12. (a) Spatiotemporal evolution of the *x*-variables shows a *Multicluster traveling chimera*. (b) Time series shows chaotic bursting. The blue curve is for the neurons of the part immersed in the field and red for the part not immersed in the electric field

3.4 Network Equations

$$\begin{cases} \dot{x}_i = y_i - a x_i^3 + b x_i^2 - z_i + I_{ext} + J_i + C_i + \mathrm{k}_1 x_i W(\phi), \\ \dot{y}_i = c - d x_i^2 - y_i, \\ \dot{\mathrm{z}}_i = r(\mathrm{s}(x_i + 1.56) - \mathrm{z}_i), \\ \dot{\phi}_i = x_i - k_2 \phi_i + \phi_{ext}. \end{cases} \tag{16}$$

$$\phi_{ext} = B_m \sin(2\pi f t) \tag{17}$$

(Lv and Ma, 2016)

a) Chimera and Multichimera state

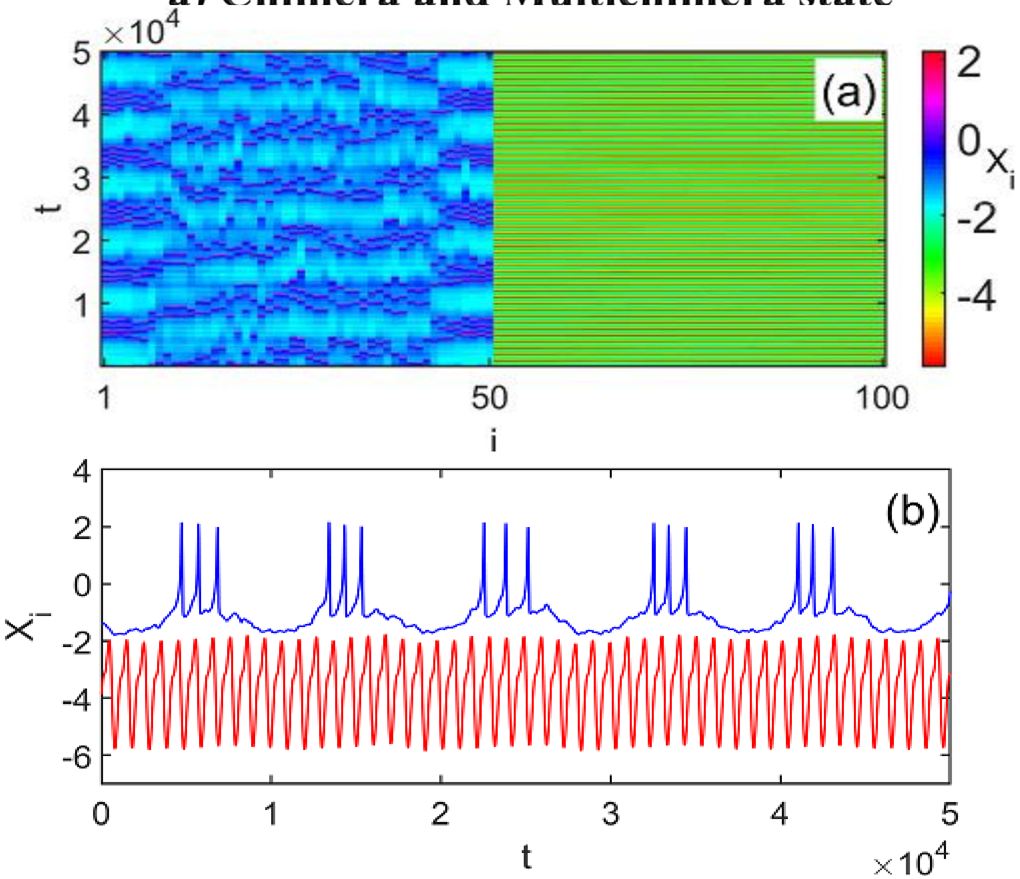

Fig23: Impact of magnetic field ($q1 = 0$ and $q2 = 9$) for $f = 0.68$. (a)Spatiotemporal evolution of the x-variables shows a *chimera state*. (b) time series shows chaotic bursting and oscillations of neurons. The red curve is for the neurons of the part immersed in the field and blue for the part not immersed in the electric field.

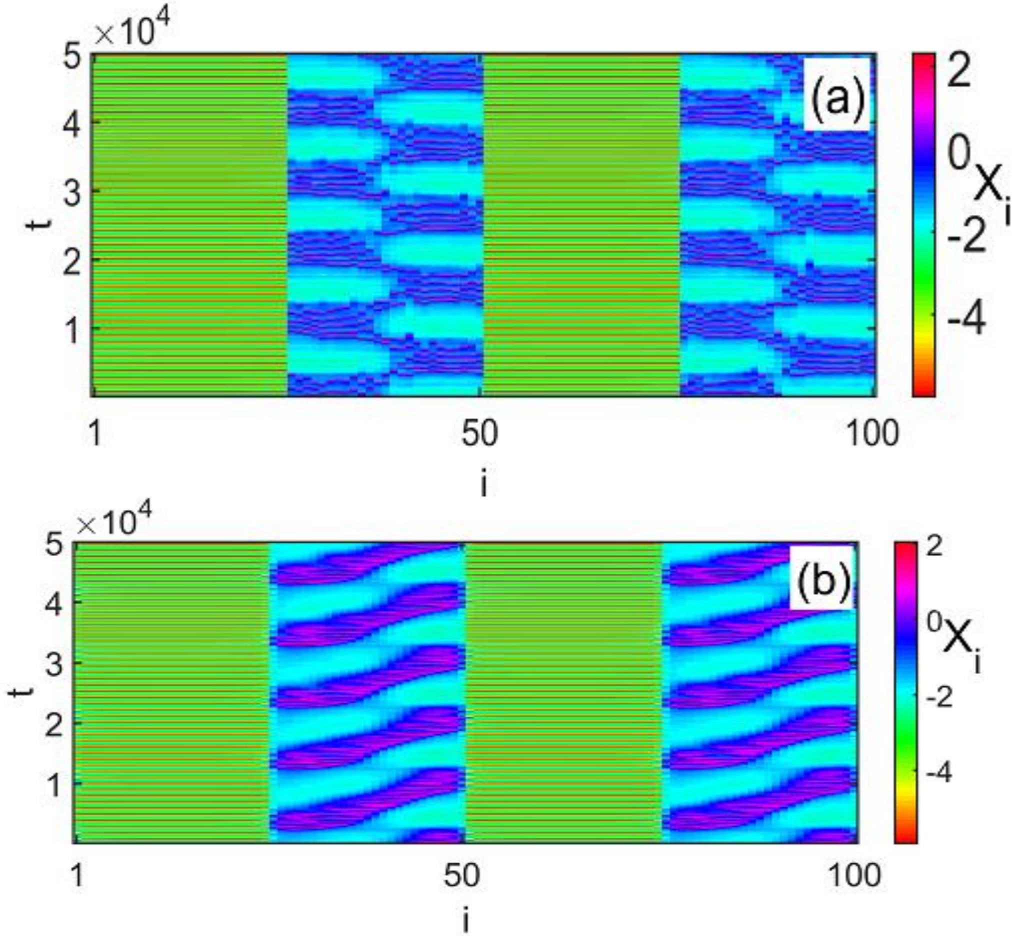

Figure 24: Multichimera state induced by magnetic field for $f = 0.68$. (a) Spatiotemporal evolution of the x-variables shows multicluster chimera state for $q1 = 0$ and $q2 = 9$. (b) Spatiotemporal evolution of the x-variables shows multicluster traveling chimera state for $q1 = 2$ and $q2 = 3$.

Network Equations

$$\begin{cases} \dot{x}_i = y_i - a x_i^3 + b x_i^2 - z_i + c_1 x_i\left(\alpha + \beta \varphi_i^2\right) + I_{ext} + J_i + C_i, \\ \dot{y}_i = c - d x_i^2 - y_i + 0.7 E_i, \\ \dot{z}_i = r(s(x_i + x_{ir}) - z_i), \\ \dot{\varphi}_i = x_i - 0.5\varphi_i + \varphi_{ext}, \\ \dot{E}_i = 0.001 y_i + E_{ext}. \end{cases} \quad (18)$$

$$B_{\max} = \sigma E_{\max} \quad (19)$$

$$\sigma = \left(\frac{n_i}{v}\right) \quad (20)$$

(Zhou and Wei, 2021)

11. Influence of electromagnetic wave on 1D-NN

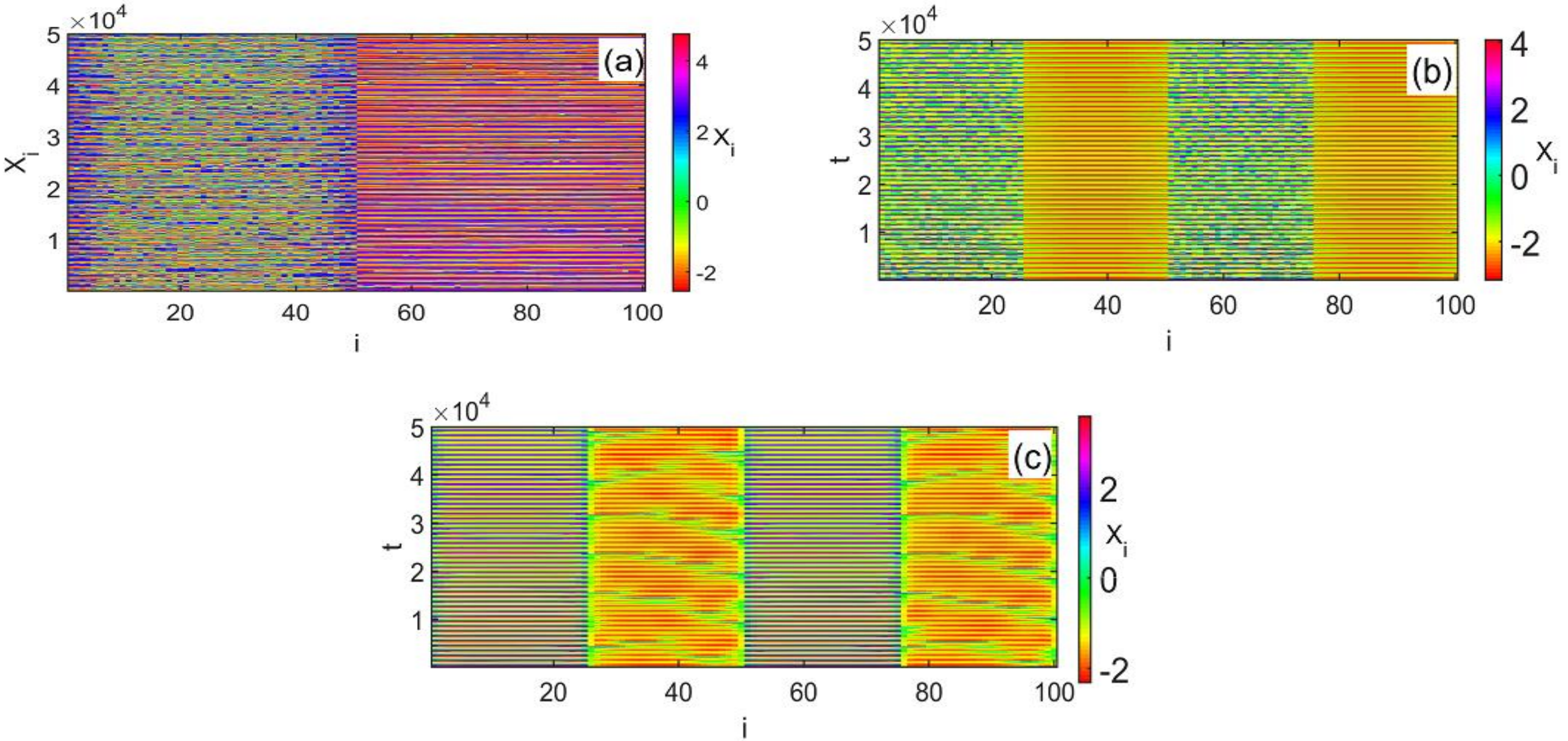

Figure25: Impact of the electromagnetic wave for f = 0.68. (a) Spatiotemporal evolution of the x-variables shows one cluster chimera state for $q1$ = 0 and $q2$ = 9 . (b) Spatiotemporal evolution of the x-variables shows multicluster chimera state for $q1$ = 0 and $q2$ = 9. (c) Spatiotemporal evolution of the x-variables shows multi traveling wave for $q1$ = 2 and $q2$ = 3.

12.Summary

Electrical field | **Magnetic field** | **Electromagnetic field**

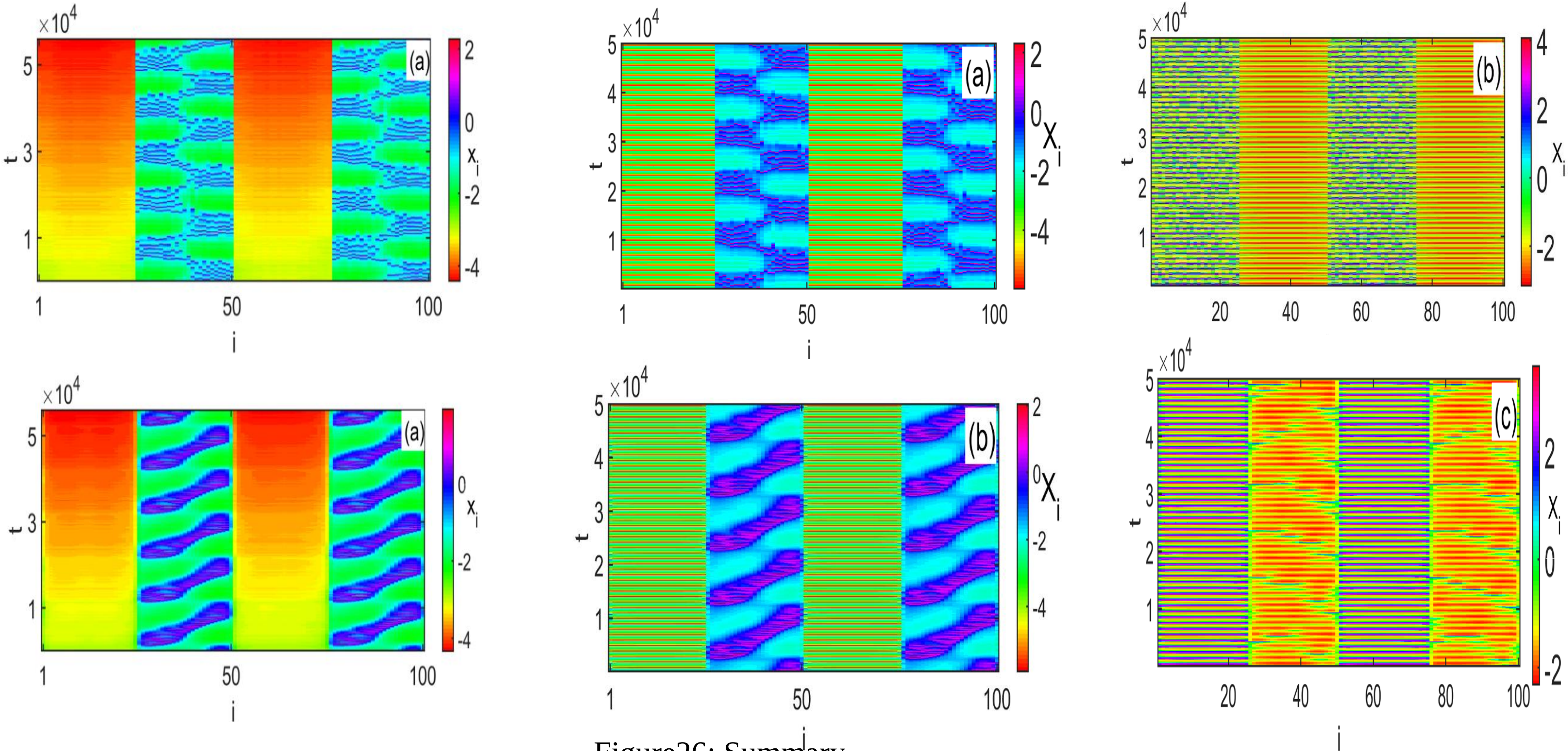

Figure26: Summary

3.Conclusion

- Highlight the phenomena appearing without external fields in a 1D network which has local electrical and nonlocal chemical couplings.

- Check for the presence of these phenomena in a larger network (2D)

- Highlight the influence of these external electromagnetic fields on the dynamics observed.

In conclusion, we can impose a variety of chimera behaviors on the network just by acting on external currents and external electromagnetic fields.

Contributors

Gaël R. Simo

Thierry Njougouo

R. P. Aristides

Patrick Louodop

Dibakar Ghosh

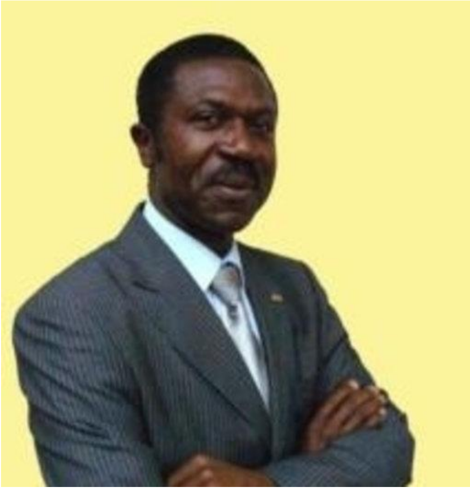

Robert Tchitnga

Hilda A. Cerdeira

❑ RELATED PAPERS

I- *Gael R. Simo, Thierry Njougouo, R. P. Aristide, Patrick Louodop, Robert Tchitnga and Hilda A. Cerdeira*(2021), " **Chimera states in a neuronal network under the action of an electric field**", ***Physical Review E*** 00, 002300.

II- *Gael R. Simo, Patrick Louodop, Dibakar Ghosh, Thierry Njougouo, Robert Tchitnga and Hilda A. Cerdeira*(2021) , "**Traveling chimera patterns in two-dimensional neuronal network**", ***Physics Letters A*** 409, 127519.

❑ CITED PUBLICATION

I- J. L. Hindmash and R.M. Rose(1984), "A Model of Neuronal Bursting Using Three Coupled First Order Differential Equations", Proc. R. Soc. London Ser. B221, 87

Thank you for your kind Attention!!!

1.2 Evolution of the Hindmarsh-Rose model

a)Two-equations model

$$\begin{cases} \dot{x} = y - ax^3 + bx^2 + I \\ \dot{y} = c - dx^2 - y. \end{cases} \qquad (1)$$

(Hindmarsh and Rose, 1982)

b)Three-equations model

$$\begin{cases} \dot{x} = y - ax^3 + bx^2 + I - z \\ \dot{y} = c - dx^2 - y \\ \dot{z} = r(s(x - x_0) - z). \end{cases} \qquad (2)$$

(Hindmarsh and Rose, 1984)

c)Four dimensional/Extended HR model

$$\begin{cases} \dot{x} = ay + bx^2 - cx^3 - dz + I \\ \dot{y} = e - fx^2 - y - g\omega \\ \dot{z} = \mu(-z + S(x + h)) \\ \dot{\omega} = \nu(-k\omega + r(y + l)). \end{cases} \qquad (3)$$

(Pinto *et al.*, 2000)

d) Hindmarsh-Rose model with electric field

$$\begin{cases} \dot{x} = y - ax^3 + bx^2 - z + I_{ext} \\ \dot{y} = c - dx^2 - y + rE \\ \dot{z} = \nu[s(x + x_0) - z] \\ \dot{E} = ky + E_{ext}. \end{cases} \qquad (4)$$

(Ma *et al.*, 2019)

e) Hindmarsh-Rose model with electromagnetic field

$$\begin{cases} \dot{x} = y - ax^3 + bx^2 - z + I_{ext} - k_1 W(\varphi)x \\ \dot{y} = c - dx^2 - y \\ \dot{z} = r[s(x + 1.6) - z] \\ \dot{\varphi} = kx - k_2\varphi + \varphi_{ext} \end{cases} \qquad (5)$$

(Lv and Ma, 2016)

$$\begin{cases} \dot{x} = y - ax^3 + bx^2 - z + I_{ext} + k_1 x(\alpha + \beta\phi^2) \\ \dot{y} = c - dx^2 - y - (1/80)\omega \\ \dot{z} = r(s(x + 1.56) - z) \\ \dot{\omega} = \nu(-\omega + e(y + 0.9)) \\ \dot{\phi} = x - k_2\phi + \phi_{ext} \end{cases} \qquad (6)$$

(Wang *et al.*, 2020b)

f) Hindmarsh-Rose model with electric and magnetic field

$$\begin{cases} \dot{x} = y - ax^3 + bx^2 - z + I_{ext} - k_1 W(\varphi)x \\ \dot{y} = c - dx^2 - y - rE \\ \dot{z} = \nu[s(x + 1.6) - z] \\ \dot{\varphi} = k_2 x - k_3\varphi + \varphi_{ext} \\ \dot{E} = k_4 y + E_{ext}. \end{cases} \qquad (7)$$

(Zhou and Wei, 2021)

5. Neuronal Network topologies under study

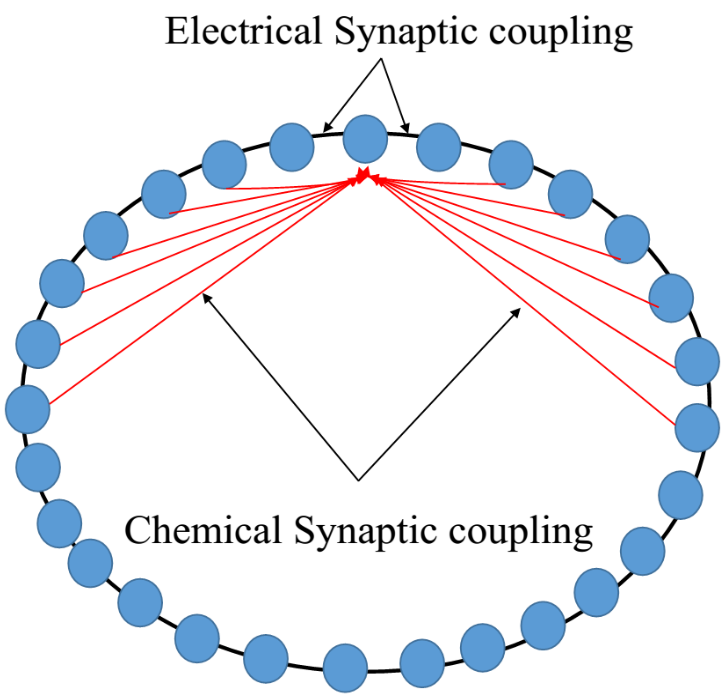

Fig2: Schematic diagram of a neuronal network. Blue dots represent HR neurons connected to their nearest neighbors by local Electrical coupling in black lines. Red lines represent non-local chemical synaptic coupling shown for one node, which is true for all other nodes.

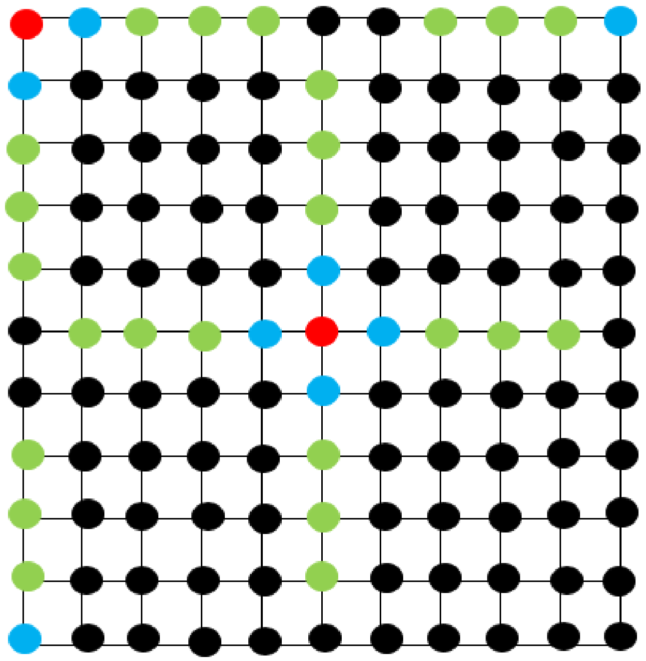

Fig3: Schematic diagram of a two-dimensional grid: the (i, j)-th node (red dot) is locally connected to four nearest-neighbors (blue circles) and non-locally connected to $p$nearest-neighbors (green circles). Black circles represent other nodes on the network. For the simple illustration, we choose $M = 11$ and $p = 4$

c) Influence of the tot al number of elements *M* of the ring

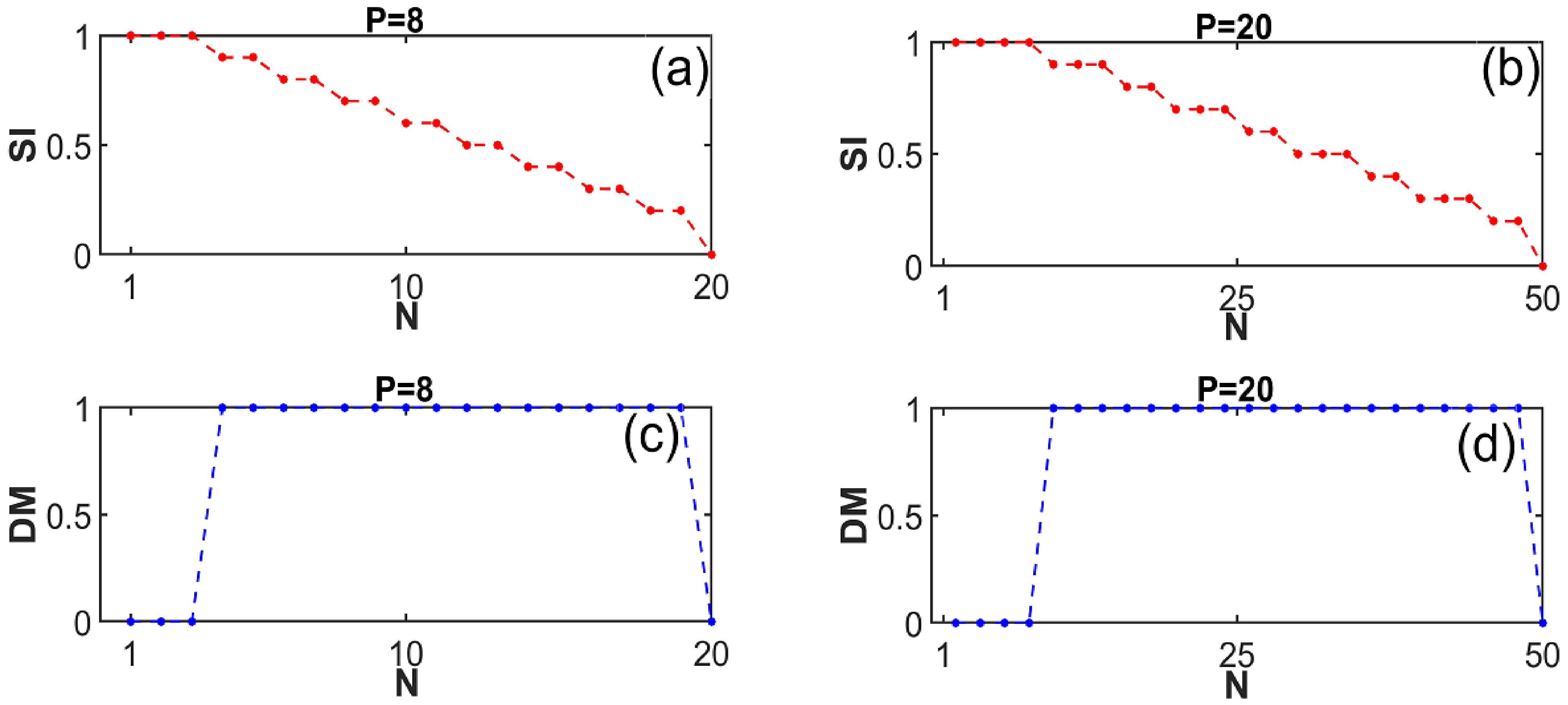

Fig 22: Influence of the number of neurons *M* of the whole ring for *f* = 12. Strength of incoherence and discontinuity measure for (a) & (c) *M* = 20, (b) & (d)*M* = 50. Appearance of the chimera state from 20% of the total number of neurons in the ring

c) Influence of the total number of elements *M* of the ring

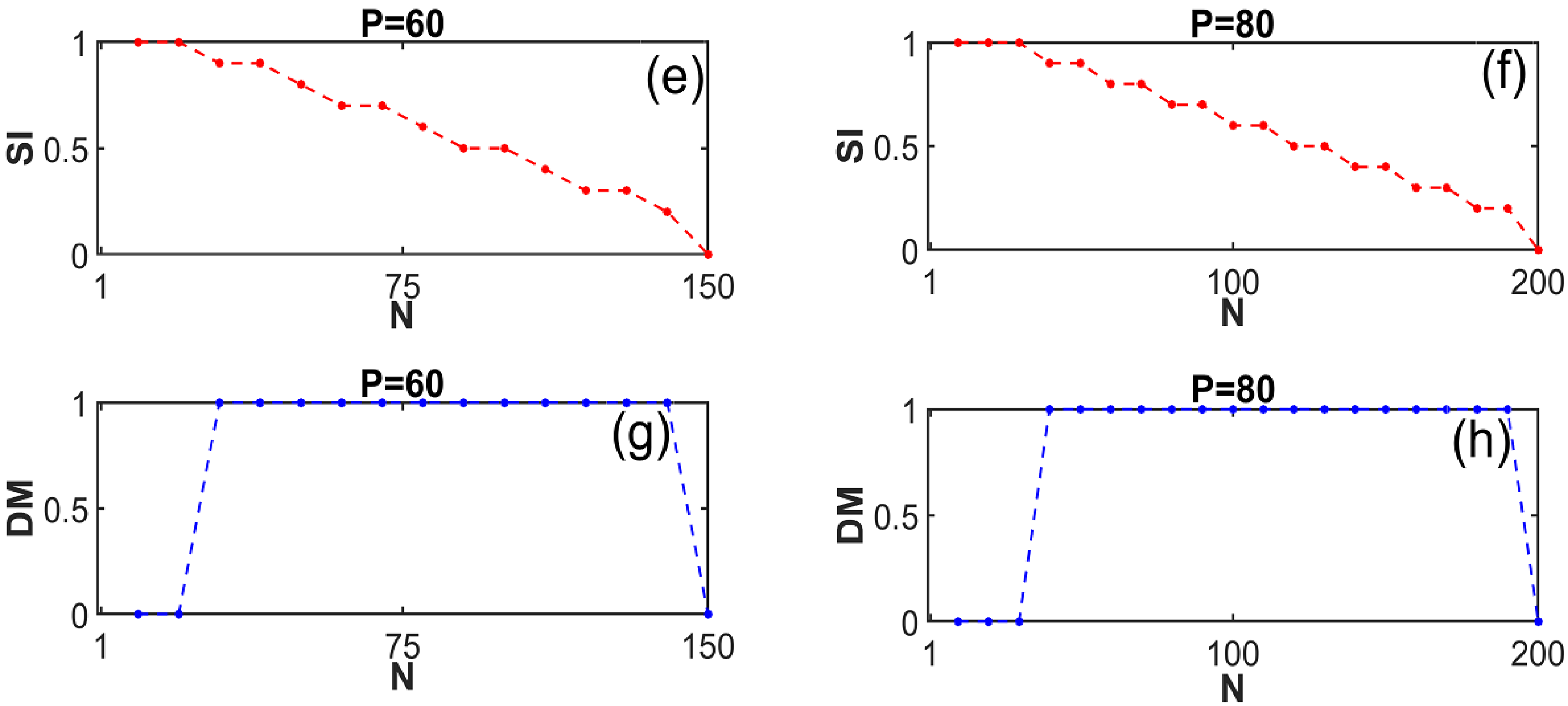

Fig 23: Influence of the number of neurons M of the whole ring for f = 12. Strength of incoherence and discontinuity measure for (e) & (g)M = 150, (f) & (h)M = 200. Appearance of the chimera state from 20% of the total number of neurons in the ring